

9201

8982 NT ACAN

NHCH
TN
2868
c.1

006589J



TECH LIBRARY KAFB, NM

NATIONAL ADVISORY COMMITTEE FOR AERONAUTICS

TECHNICAL NOTE 2868

LOAN COPY: RETURN TO
AFWL TECHNICAL LIBRARY
KIRTLAND AFB, N.M.

REFLECTION OF A WEAK SHOCK WAVE FROM A BOUNDARY
LAYER ALONG A FLAT PLATE

I - INTERACTION OF WEAK SHOCK WAVES
WITH LAMINAR AND TURBULENT BOUNDARY LAYERS
ANALYZED BY MOMENTUM-INTEGRAL METHOD

By Alfred Ritter and Yung-Huai Kuo

Cornell University



Washington

January 27, 1953

AFMDC
TECHNICAL LIBRARY
AFL 2811

NATIONAL ADVISORY COMMITTEE FOR AERONAUTICS

TECHNICAL NOTE 2868

REFLECTION OF A WEAK SHOCK WAVE FROM A BOUNDARY
LAYER ALONG A FLAT PLATEI - INTERACTION OF WEAK SHOCK WAVES
WITH LAMINAR AND TURBULENT BOUNDARY LAYERS
ANALYZED BY MOMENTUM-INTEGRAL METHOD

By Alfred Ritter and Yung-Huai Kuo

SUMMARY

The present paper is concerned with the phenomena encountered when a plane oblique shock wave is incident upon the boundary layer of a flat plate. In an effort to simplify the problem, the flow field was divided into a viscous layer near the wall and a supersonic potential outer flow. The pressure disturbances due to the incident wave would be propagated upstream and downstream in the subsonic portion of the boundary layer, thus giving rise to perturbations of the boundary layer. By restricting the study to infinitesimal incident compression waves, only small perturbations were encountered and hence the ordinary linearized theory could be applied to the outer flow. In the laminar case, the boundary-layer treatment was based upon a momentum-integral equation previously derived by Howarth. The two flows must be compatible; hence, the deflection of the streamlines near the boundary layer was expressed in terms of the vertical velocity component along the edge of the boundary layer and this relation was used as a boundary condition for the outer flow. The boundary condition determined the form of solution upstream and downstream of the point of incidence. Determination of the constants of integration was accomplished by a consideration of conditions at infinity and a matching of the two flows at the point of incidence. With the outer flow thus determined, boundary-layer growth and pressure distribution were computed and results for the laminar case were obtained as follows:

- (a) The pressure disturbance along the wall decreased exponentially from a definite value at the point of incidence to zero far upstream of the point of incidence. Downstream of the point of incidence, the pressure rose to a maximum value and then dropped off to the value corresponding to regular reflection.

(b) The disturbances produced by the interaction decayed exponentially upstream; for a free-stream Mach number of approximately 2 and a Reynolds number of approximately 1500 in the undisturbed boundary-layer displacement thickness the upstream influence was of the order of 30 boundary-layer displacement thicknesses.

(c) The "self-induced" pressure gradient along the wall was such that the boundary layer might separate ahead of the point of incidence. If separation occurred, the separation point moved upstream as the shock strength was increased. With increasing Reynolds number, the separation point also moved upstream, whereas for increasing Mach number, the separation point moved downstream.

In the turbulent case the upstream influence was quite small and the incident wave must be reflected as a shock wave.

INTRODUCTION

It has been found that if the free-stream subsonic Mach number becomes high enough so that local supersonic zones are formed on an airfoil, sharp changes in the airfoil characteristics occur which cannot be explained by classical aerodynamics. The resulting loss of lift is accompanied by a large increase of drag in consequence of the appearance of shock waves on the surface of the airfoil. However, close study reveals that the drag increase is too large to be accounted for by the shock loss and change in skin friction. It must be caused by the sudden change of the flow pattern. This seems to indicate that the shock wave, when formed over the airfoil surface, modifies the character of the boundary layer in such a way as to create a wider wake.

At Guidonia, Ferri, by examining the measured pressure distributions over airfoils at supersonic speeds, found that for the forward portions of the airfoil the experimental pressure distribution agrees quite well with that calculated from potential-flow theory (reference 1). As the trailing edge is approached, however, the experimental pressures along the upper surface, for positive angles of attack, become considerably higher than the calculated ones. (At negative angles of attack, this behavior occurs along the lower surface.) This discrepancy is understandable in the light of the fact that the boundary layer on the rear portion of the airfoil is extremely sensitive to pressure disturbances. Since the flow far away from the airfoil has to return to its original pressure and direction, a shock wave must emanate at or near the trailing edge. There is a sharp pressure rise across the shock and pressure disturbances are transmitted upstream in the subsonic portion of the boundary layer causing a thickening of the layer near the trailing edge. This thickening, in turn, generates compression waves which travel downstream

and interact with the shock wave. The net result is that there is, starting from some point forward of the trailing edge, a gradual compression to the main-stream pressure. The pressure distribution is hence altered in such a manner as to give values of lift and pressure drag smaller than those calculated from theory. The measured moment coefficient will also differ from the theoretical values.

The preceding discussion shows that, in the transonic and supersonic regimes, the Mach number alone is insufficient to determine the flow characteristics; the Reynolds number can also be important. This was first demonstrated by Ackeret, Feldmann, and Rott in experiments which established the close relationship between the shock-wave pattern and the Reynolds number (reference 2). These prove beyond doubt that the flow far away from the wall depends intimately upon the character of the boundary layer, that is, the Reynolds number. Thus, under such circumstances, the concept of the boundary layer requires modification.

As a first step, a simplified problem of a plane shock wave incident upon the laminar boundary layer over a flat surface will be dealt with. For a number of years, Dr. H. W. Liepmann and his associates at the California Institute of Technology have been conducting experimental studies of shock-wave boundary-layer interaction. Recently they investigated the problem of the reflection of shock waves from boundary layers (reference 3). Based on the qualitative experimental data, some important conclusions were drawn regarding the reflection of an incident shock wave from a boundary layer:

(a) The type of boundary layer, whether laminar or turbulent, markedly affects the interaction. With a turbulent boundary layer, the reflection is practically the same as that for a regular reflection in nonviscous flow theory. For a laminar boundary layer, however, there is a large interaction zone near the point of incidence that is quite different from the regular inviscid reflection. The incident wave is apparently reflected as from a constant-pressure surface in the form of a Prandtl-Meyer fan. In returning to its final direction parallel to the wall, the deflected flow, behind the expansion, recompresses to the pressure appropriate to that behind a regular reflection.

(b) For $M = 1.4$ and $Re_x = \frac{Ux}{\nu_\infty} = 0.9 \times 10^6$, the influence of the incident wave extends upstream in a laminar layer a distance of the order of 50 boundary-layer displacement thicknesses. On the other hand, the upstream influence is practically negligible for the turbulent boundary layer.

(c) It appears that, except for very weak incident waves, the laminar layer almost always separates somewhere in front of the point of incidence, whereas no separation was found for the turbulent layer.

Quite recently, Barry, Shapiro, and Neumann (reference 4) made a similar study and their results are in substantial agreement with the GAIT results. An advantage of their experiments, however, is that, although the tests were carried out at constant Mach number, the Reynolds number and shock strength were varied so that more qualitative as well as quantitative data are available to serve as a guide to future theoretical work.

Theoretical solutions of this problem have been almost as meager as the experimental results. A first attempt was made by Howarth (reference 5), who considered the case of a wave incident upon the interface bounding two semi-infinite uniform streams, one supersonic and one subsonic. Viscosity and heat conduction were neglected and the equations were linearized. He then demonstrated the upstream propagation of disturbances in the subsonic portion of the flow field and showed that an incident compression wave is reflected as compression upstream of the point of incidence while being reflected as expansion downstream of the point of incidence. However, these results can only be regarded as qualitative because of the obvious shortcomings of the model. In an effort to make the Howarth model more realistic, Tsien and Finston simulated the boundary layer with a uniform subsonic stream bounded by a wall on one side and a semi-infinite, uniform, supersonic stream on the other (reference 6). As before, viscosity and heat conduction were neglected and only small disturbances were considered. For the case of a compression wave incident upon the interface separating the two streams, it was shown that except for the local interaction, the incident compression wave is regularly reflected. Locally, however, the pressure along the interface exhibits compression ahead of the point of incidence and expansion immediately behind it. This local condition is qualitatively the same as that observed in experiments with shock reflection from laminar boundary layers; consequently there arose the speculation that perhaps the effects of viscosity and heat conduction were actually not too important in comparison with the effect of coexistence of supersonic and subsonic streams. If this were the case, it should follow that an improvement in the Tsien-Finston model could give rise to more quantitative results. Now an obvious discrepancy between the Tsien-Finston model and the physical situation is that the uniform subsonic stream, in attempting to simulate the boundary layer, is incapable of satisfying the "no-slip" condition at the wall. Thus, the next logical step in the development of the theory would appear to be that of considering a main-stream velocity that varies from zero at the wall to a given uniform supersonic velocity a short distance from the wall, and, in fact, this has been considered by Robinson (reference 7) and Lighthill (reference 8). Robinson assumed that the main-stream velocity varies continuously from zero at the wall to supersonic velocity some distance from the wall, whereas Lighthill assumed that the Mach number varies from zero at the wall to some supersonic value a short distance from the wall. A weak wave is incident upon the boundary layer and the reflected waves and upstream

influence were evaluated. Now with the improved model, however, both investigators found, contrary to experimental evidence, that the upstream influence is negligible. Although Robinson was chiefly concerned with the determination of the upstream influence, Lighthill considered, in some detail, the local reflection of the shock wave. He concluded that a shock is reflected locally as a "pressure ridge," that is, a rapid compression followed immediately by a rapid expansion. Now a note was added in the proof of reference 8 to the effect that experimental results of Mair and Bardsley (reference 9), obtained at the Fluid Motion Laboratory, Manchester, establish that the conclusions of negligible upstream influence and the shock being locally reflected as a pressure ridge are correct for the reflection of a weak shock from a turbulent boundary layer. (These results, however, had been previously observed by Ackeret and Liepmann.) As Lighthill pointed out, the conjecture that the theory is correct for velocity profiles typical of turbulent boundary layers but incorrect for profiles typical of laminar boundary layers may be valid. But until such time as the theory is modified to account for viscosity, as suggested by Lighthill, the present theory is incapable of predicting the effects of the interaction between a shock wave and a laminar boundary layer.

The preceding theories have neglected viscosity and heat conduction while considering infinitesimal waves and small disturbances. It would appear that the assumption of infinitesimal waves and small disturbances is valid since the linear theory, to be a good approximation, requires that the slopes of the streamlines be small. For weak incident shock waves, the slope of the displacement thickness would probably be small, except perhaps in the immediate vicinity of the wave. The neglect of viscosity, on the other hand, seems to be more serious. If the effects of viscosity were not too important, one would expect that, for fixed Mach number and shock strength, the effect of Reynolds number should be rather small. Actually, this is not the case since the results of Barry, Neumann, and Shapiro clearly show that changes in Reynolds number have a marked effect upon the shock-wave - laminar-boundary-layer interaction (reference 4). Hence it appears that a theory capable of predicting the effects of this complicated phenomenon must include the effects of viscosity.

At present, as far as the authors are aware, the only solution that includes viscous effects was given by Lees (reference 10). The Lees theory is based on an approximate relationship between the slope of the displacement thickness and the external pressure gradient derived from Prandtl-Meyer flow. By combining this relation with the momentum-integral equation and neglecting terms of the order of Re^{-1} Lees arrived at a third-order, linear, differential equation for the pressure. On the assumption that this equation is valid all along the boundary layer, he was able to determine the boundary-layer growth and pressure distribution. He found the upstream influence comparable with that which is observed

experimentally and showed, also, that the boundary layer always separates except in those cases where the incident wave is quite weak. However, his theoretical pressure distributions fail to exhibit the characteristic downstream behavior. This point will be discussed later.

Following the approach of Oswatitch and Wiegardt in their study of the growth of disturbances in a supersonic stream outside laminar or turbulent boundary layers (reference 11), the problem is treated as an outer flow, with a shock, in equilibrium with a boundary-layer flow. Instead of expressing the deflection of the streamline in terms of pressure rise, as in Lees' problem, a procedure after Oswatitch and Wiegardt is taken by connecting the vertical velocity of the outer flow with the streamline deflection, as given by the momentum integral of the boundary-layer flow. This reduces the problem to an inviscid one which can be solved systematically to any order of approximation.

This study was conducted at the Graduate School of Aeronautical Engineering of Cornell University under the sponsorship and with the financial assistance of the National Advisory Committee for Aeronautics.

SYMBOLS

a	speed of sound
A, B, C, D, E	constants
$b = \delta_1^* / \delta_0^*$	
c_p, c_v	specific heats at constant pressure and constant volume, respectively
f, g	functions of $\xi - m_\infty \eta$ and $\xi + m_\infty \eta$, respectively
$F = 2\eta - 2\eta^3 + \eta^4$	
g_1, g_2, g_3, g_4	defined by equations (8)
$G = \frac{1}{6}\eta(1 - \eta)^3$	
h	function of $\xi - m_\infty \eta$
$H \equiv \delta^* / \theta$	

k	coefficient of thermal conductivity
K	Kármán momentum equation for compressible viscous fluids
$m = \sqrt{M^2 - 1}$	
M	Mach number (U/a)
$M_0 = U/a_0$	
$M_\infty = U/a_\infty$	
p	pressure
p'	perturbed pressure
Pr	Prandtl number ($\mu c_p/k$)
R	universal gas constant
Re	Reynolds number ($U\delta_0^*/\nu_0$)
$Re_x = U_x/\nu_0$	
T	temperature
u, v	velocity components parallel and normal to flow direction, respectively
u', v'	velocity perturbations nondimensionalized with U
U	free-stream velocity
x, y	coordinates parallel and normal to flow direction, respectively
x', y'	values of x and y in transformed plane ($x' = x$; $y' = \left(\frac{p}{p_0}\right)^{1/2} \int_0^y \frac{T_0}{T} dy$)
α	constant
$\beta \equiv \sigma^{\frac{3-2\gamma}{\gamma-1}} / \left(\frac{37}{315} - \frac{263}{630\sigma} \right)^2$	

0

γ	ratio of specific heats (c_p/c_v)
δ	boundary-layer thickness
δ^*	boundary-layer displacement thickness
δ_o^*	undisturbed boundary-layer displacement thickness
δ'	boundary-layer thickness in transformed plane
δ'^*	boundary-layer displacement thickness in transformed plane
Δ	disturbed boundary-layer displacement thickness nondimensionalized with δ_o^*
ϵ	flow-deflection angle
$\eta = y/\delta'$ or y/δ_o^*	
θ	boundary-layer momentum thickness $\left(\int_0^\delta \left(1 - \frac{u}{u_e} \right) \frac{\rho u}{\rho_e u_e} dy \right)$
θ'	boundary-layer momentum thickness in transformed plane
$\lambda_1, \lambda_2, \lambda_3$	roots of equation (16)
$\Lambda = \frac{(\delta')^2}{v_o} \left(1 + \frac{\gamma - 1}{2} M_e^2 \right) \frac{du_e}{dx}$	
μ	coefficient of viscosity
ν	kinematic coefficient of viscosity
$\xi = x/\delta_o^*$	
ρ	density
$\sigma = 1 - \frac{\gamma - 1}{2} M_o^2 = \left(1 + \frac{\gamma - 1}{2} M_\infty^2 \right)^{-1}$	
τ	shear stress
ϕ	perturbation velocity potential, nondimensionalized with $U\delta_o^*$

ϕ	total potential
χ	function of x' and y'
ψ	stream function
Subscripts	
d	evaluated at distance of upstream influence
e	evaluated along edge of boundary layer
i	1, 2, or 3
l	laminar case
o	standard condition, such as stagnation point or undisturbed state
s	separation point
t	turbulent case
w	evaluated at wall
$1,2,3$	evaluated in regions 1, 2, or 3, respectively (see fig. 1)
∞	evaluated in undisturbed free stream

OUTLINE OF PRESENT INVESTIGATION

In the present study the effect of an infinitesimal compression wave incident upon the laminar boundary layer along a flat plate in supersonic flow will be considered. The pressure gradient in the flow direction is determined to the order of approximation of the ordinary boundary-layer theory solely by the shape of the boundary. The potential flow thus completely determines the boundary-layer growth. In the problem of interaction between a shock wave and a boundary layer, however, the phenomena are quite different. In that case the pressure disturbances that are propagated upstream in the subsonic portion of the boundary layer will affect the boundary-layer growth. It becomes clear that the outer flow influences the boundary-layer growth and that the boundary-layer growth, in turn, influences the outer flow, so that a solution that is simultaneously compatible with the two flows must be sought.

Another significant difference between the interaction and noninteraction problems occurs in the separation phenomenon. For the usual case of boundary-layer flow against a pressure gradient, it is known that the

flow separates from the wall at the point where $\left(\frac{\partial u}{\partial y}\right)_w = 0$. Downstream

of the separation point the original flow is deflected away from the wall by the backflow, a vortex layer separating the two flows. The interaction of a shock wave with a laminar boundary layer, however, produces a different form of separation. Experimental evidence indicates that along the wall there exists a short thin region, extending slightly upstream from the foot of the shock wave, in which the flow has practically zero velocity; the boundary between this separated flow and the main boundary-layer flow is a vortex sheet. A plausible explanation of this phenomenon is proposed by Lighthill, who suggests that the pressure discontinuity occurring when a shock interacts with a laminar boundary layer causes the flow to separate into some form of "bubble" at the base of the shock wave. Once such a bubble is produced, the boundary layer upstream of the separated region will be deflected so as to increase the external pressure gradient. This results in further separation of the boundary layer and hence further upstream deflection. This process of repeated separation causes the edge of the bubble to move upstream until such time as the induced pressure gradient is no longer able to cause separation of the boundary layer. The net result is the one indicated in experiments. Immediately behind the point of interaction, the deflected flow, in returning to its original direction parallel to the wall, undergoes a very rapid compression, thereby causing an extremely large pressure gradient. It is known from experimental results that the boundary layer downstream is turbulent, but whether the extreme pressure gradient causes separation and hence causes the boundary layer to become turbulent or whether the flow at that point is already turbulent and thus can sustain large pressure gradients must remain at this time a matter of conjecture. Whatever the case may be, in the problem for weak shock the flow will be assumed to remain laminar downstream of the point of incidence (cf. reference 12). Positive infinity in relation to the problem will be taken to mean a distance downstream of the order of 100 boundary-layer thicknesses. In addition, any mention of boundary-layer separation will refer to the "dead air bubble" phenomenon.

In the present theory it is assumed that the boundary-layer equations are applicable over the whole plane. Strictly speaking, the validity of the usual boundary-layer assumptions near the base of the shock wave is doubted, since separation occurs. However, it is believed that for weak incident waves, a theory based on the above assumptions will still enable one to determine some of the important characteristics of the flow. In particular it is desired to determine the extent of the separated region, since this investigation is merely the first step of a proposed theory which will endeavor to take separation into account.

The more refined theory is then expected to furnish, in the separation zone, slight corrections to the simplified theory.

The flow field is assumed to be divided into two distinct regions as follows:

- (a) A thin layer adjacent to the plate wherein there is laminar-type boundary-layer flow
- (b) An outer supersonic potential flow field

Since an infinitesimal compression wave is assumed, the upstream pressure propagation is expected to perturb the boundary layer just slightly, thus imposing small disturbances upon the outer flow. This justifies the linearization of the supersonic outer flow. (Results of this theory will of course be applicable only for fairly weak shock waves.) The flow field has been assumed to be separated into two distinct regions. In reality a continuous variation in velocity from zero at the boundary to some main-stream value a short distance from the wall is known to exist. The actual distance at which the velocity reaches its main-stream value is rather indefinite; hence the so-called boundary-layer displacement thickness $\delta^*(x)$ is defined. Physically it represents how much the potential flow streamlines are deflected because of the reduction in mass flow caused by the retarded velocities near the wall. The viscous effects are thus characterized by a layer whose thickness is $\delta^*(x)$, and the link connecting the outer flow to the boundary-layer flow is the condition that the line $y = \delta^*(x)$ is a streamline of the outer flow. The treatment of the boundary layer in the present study is based upon a momentum-integral equation previously derived by Howarth (reference 13). The deflection of the boundary layer is expressed in terms of the vertical velocity component along the edge of the layer and this relation is used as a boundary condition for the outer flow. Hence the over-all problem is then reduced to the solution of a purely supersonic potential-flow problem.

LAMINAR-BOUNDARY-LAYER EQUATIONS

The Prandtl boundary-layer equations for the two-dimensional steady flow of a viscous compressible fluid are:

$$u \frac{\partial u}{\partial x} + v \frac{\partial u}{\partial y} = -\frac{1}{\rho} \frac{\partial p}{\partial x} + \frac{1}{\rho} \frac{\partial}{\partial y} \left(\mu \frac{\partial u}{\partial y} \right)$$

$$0 = -\frac{1}{\rho} \frac{\partial p}{\partial y}$$

$$\frac{\partial}{\partial x}(\rho u) + \frac{\partial}{\partial y}(\rho v) = 0$$

$$\rho c_p \left(u \frac{\partial T}{\partial x} + v \frac{\partial T}{\partial y} \right) = u \frac{\partial p}{\partial x} + \mu \left(\frac{\partial u}{\partial y} \right)^2 + \frac{\partial}{\partial y} \left(k \frac{\partial T}{\partial y} \right)$$

$$p = R\rho T$$

Here u and v denote, respectively, the x and y components of the velocity and p , ρ , and T , the pressure, density, and temperature of the fluid. In order to simplify the problem, Howarth (reference 13) assumes that the coefficient of viscosity μ is proportional to the temperature and the Prandtl number is unity. These assumptions, of course, introduce some approximation, but according to the results of Emmons and Brainerd (references 14 and 15), the boundary-layer characteristics depend very insensitively on the form of $\mu(T)$ and the change of Prandtl number for moderate Mach numbers. Therefore, the simplifications brought about by this assumption justify the slight loss in accuracy.

By introduction of the stream function ψ

$$\rho u = \rho_0 \frac{\partial \psi}{\partial y}$$

$$\rho v = -\rho_0 \frac{\partial \psi}{\partial x}$$

and by introduction of the transformation

$$x' = x$$

$$y' = \left(\frac{p}{p_0} \right)^{1/2} \int_0^y \frac{T_0}{T} dy$$

$$\psi = \left(\frac{p}{p_0} \right)^{1/2} \chi(x', y')$$

the momentum equation is transformed into

$$\frac{\partial^2 \chi}{\partial x' \partial y'} \frac{\partial \chi}{\partial y'} - \frac{\partial^2 \chi}{(\partial y')^2} \frac{\partial \chi}{\partial x'} = u_e \frac{du_e}{dx'} \left[\frac{T}{T_e} - \frac{\gamma}{2a_e^2} \chi \frac{\partial^2 \chi}{(\partial y')^2} \right] + \nu_0 \frac{\partial^3 \chi}{(\partial y')^3}$$

where ρ_0 , T_0 , and ν_0 stand for the density, temperature, and kinematic viscosity of a standard condition, the stagnation point, say, and are constants, and the subscript e indicates the condition at the edge of the boundary layer. In the case of a thermally insulated plate

$\left(\frac{\partial T}{\partial y} \right)_w = 0$, the condition of unity Prandtl number admits a special solution on the plate (reference 16)

$$c_p T + \frac{1}{2} u^2 = c_p T_e + \frac{1}{2} u_e^2$$

Upon elimination of T , there results the equation:

$$\frac{\partial^2 \chi}{\partial x' \partial y'} \frac{\partial \chi}{\partial y'} - \frac{\partial^2 \chi}{(\partial y')^2} \frac{\partial \chi}{\partial x'} = \nu_0 \frac{\partial^3 \chi}{(\partial y')^3} + u_e \frac{du_e}{dx'} \left\{ 1 + \frac{\gamma - 1}{2a_e^2} \left[u_e^2 - \left(\frac{\partial \chi}{\partial y'} \right)^2 \right] - \frac{\gamma}{2a_e^2} \chi \frac{\partial^2 \chi}{(\partial y')^2} \right\} \quad (1)$$

Thus, it is seen that when $\frac{du_e}{dx} = 0$, that is, at constant pressure, this equation is identical to the equation for the incompressible fluid.

Let δ' be the boundary-layer thickness in the transformed plane, and define the corresponding displacement and momentum thicknesses by

$$\delta'^* = \int_0^{\delta'} \left(1 - \frac{u}{u_e} \right) dy'$$

$$\theta' = \int_0^{\delta'} \left(1 - \frac{u}{u_e} \right) \frac{u}{u_e} dy'$$

Then, by integrating equation (1) across the boundary layer, the equation relating the boundary-layer thicknesses with the velocity is

$$\frac{d\theta'}{dx'} + \left[\left(2 - \frac{u_e^2}{2a_e^2} \right) \theta' + \left(1 + \frac{\gamma - 1}{2} \frac{u_e^2}{a_e^2} \right) \delta'^* \right] \frac{1}{u_e} \frac{du_e}{dx'} = \frac{v_o}{u_e^2} \left(\frac{\partial u}{\partial y'} \right)_w \quad (2)$$

The similarity of this equation to that of the incompressible flow suggests the applicability of the Kármán-Pohlhausen procedure.

If the velocity profile is given by (reference 13)

$$\frac{u}{u_e} = F(\eta) + \Lambda G(\eta)$$

where

$$F = 2\eta - 2\eta^3 + \eta^4$$

$$G = \frac{1}{6} \eta(1 - \eta)^3$$

$$\Lambda = \frac{(\delta')^2}{v_o} \left(1 + \frac{\gamma - 1}{2} M_e^2 \right) \frac{du_e}{dx}$$

with

$$\eta = \frac{y'}{\delta'}$$

$$M_e = \frac{u_e}{a_e}$$

it follows that

$$\left. \begin{aligned} \theta' &= \frac{\delta'}{315} \left(37 - \frac{\Lambda}{3} - \frac{5\Lambda^2}{144} \right) \\ \delta'^* &= \frac{\delta'}{120} (36 - \Lambda) \\ \left(\frac{\partial u}{\partial y'} \right)_w &= \frac{u_e}{\delta'} \left(2 + \frac{\Lambda}{6} \right) \end{aligned} \right\} \quad (3)$$

Substitution of the quantities of equations (3) into equation (2) gives rise to a relation between the boundary-layer thickness δ' and the velocity $u_e(x)$, with a parameter Λ . Now, in the present problem, as the flow in the boundary layer must be compatible with the potential field, the flow deflection $d\delta^*/dx$ of the boundary layer determines the flow in the outer field. Therefore, δ' should be eliminated. For this purpose, let the displacement thickness be introduced:

$$\delta^* = \int_0^{\delta} \left(1 - \frac{\rho u}{\rho_e u_e}\right) dy$$

But in the transformed plane there is

$$\begin{aligned} \delta'^* &= \int_0^{\delta'} \left(1 - \frac{u}{u_e}\right) dy' \\ &= \left(\frac{p}{p_o}\right)^{1/2} \int_0^{\delta} \frac{T_o}{T} \left(1 - \frac{u}{u_e}\right) dy \\ &= \left(\frac{p}{p_o}\right)^{1/2} \frac{T_o}{T_e} \int_0^{\delta} \left[\left(\frac{T_e}{T} - 1\right) + \left(1 - \frac{\rho u}{\rho_e u_e}\right) \right] dy \end{aligned}$$

By means of the temperature-velocity relation and Pohlhausen's profile this will yield

$$\delta'^* = \left(\frac{p}{p_o}\right)^{1/2} \frac{T_o}{T_e} \delta^* + \frac{\gamma - 1}{2} M_e^2 \left(-1 + \frac{367}{630} + \frac{1}{3} \frac{71}{2520} \Lambda + \frac{1}{252} \frac{\Lambda^2}{36} \right) \delta'$$

Now, from the second of equations (3), δ'^* is already expressed in terms of δ' and Λ . The elimination of δ'^* then gives

$$\begin{aligned} &\frac{\gamma - 1}{72} \frac{M_e^2}{252} \left[\frac{1}{v_o} \frac{du_e}{dx} \left(1 + \frac{\gamma - 1}{2} M_e^2\right) \right]^2 (\delta')^5 + \\ &\frac{1}{v_o} \frac{du_e}{dx} \left(1 + \frac{\gamma - 1}{2} M_e^2\right) \left(\frac{\gamma - 1}{6} \frac{71 M_e^2}{2520} + \frac{1}{120} \right) (\delta')^3 + \\ &\left(\frac{\gamma - 1}{2} \frac{367 M_e^2}{630} - \frac{\gamma - 1}{2} M_e^2 - \frac{3}{10} \right) \delta' = - \left(\frac{p}{p_o}\right)^{1/2} \frac{T_o}{T_e} \delta^* \end{aligned} \quad (4)$$

Theoretically, this equation defines δ' as a function of δ^* . Only in the case of small pressure gradient, namely,

$$u_e = U(1 + u' + \dots)$$

$$u' \ll 1$$

however, is a simple analytical solution possible. For by retaining only linear terms in u' and its derivatives there is obtained (reference 17)

$$\begin{aligned} \frac{U}{v_o} \left(\frac{1}{3} \frac{71}{2520} \sigma^{-2} - \frac{\sigma^{-1}}{945} \right) \frac{du'}{dx} (\delta')^3 + \left[\frac{37}{315} - \frac{263}{630\sigma} - \frac{263}{630} \frac{(\gamma - 1)M_o^2}{\sigma^2} u' \right] \delta' = \\ \left[\frac{2-\gamma}{\sigma^{2(\gamma-1)}} - \frac{2-\gamma}{2} M_o^2 \sigma^{\frac{4-3\gamma}{2(\gamma-1)}} u' \right] \delta^* \end{aligned} \quad (5)$$

where $M_o = \frac{U}{a_o}$ and $\sigma = 1 - \frac{\gamma-1}{2} M_o^2$. Moreover, since u' is assumed to be small, that is, for weak interaction, the boundary-layer thickness δ' must also differ from the unperturbed value by a small amount. Therefore, to the first-order approximation there results the solution:

$$\begin{aligned} \delta' = \sigma^{\frac{2-\gamma}{2(\gamma-1)}} \left(-\frac{37}{315} + \frac{263}{630\sigma} \right)^{-1} \delta^* - \\ \left[\frac{263}{630} \frac{(\gamma-1)M_o^2}{\sigma^{\frac{6-5\gamma}{2(\gamma-1)}}} \left(\frac{263}{630\sigma} - \frac{37}{315} \right)^{-2} + \frac{2-\gamma}{2} M_o^2 \sigma^{\frac{4-3\gamma}{2(\gamma-1)}} \left(\frac{263}{630\sigma} - \frac{37}{315} \right)^{-1} \right] u' \delta^* + \\ \frac{U}{v_o} \left(\frac{1}{3} \frac{71\sigma^{-2}}{2520} - \frac{\sigma^{-1}}{945} \right) \left(\frac{263}{630\sigma} - \frac{37}{315} \right)^{-4} \sigma^{\frac{3(2-\gamma)}{2(\gamma-1)}} \frac{du'}{dx} (\delta^*)^3 \end{aligned} \quad (6)$$

Let δ_o^* be the unperturbed displacement thickness and write

$$\delta^* = \delta_o^* (1 + \Delta)$$

Substituting equation (6) in the momentum equation (2), replacing x' by x , and keeping only first-order terms, one obtains, by taking into account $\delta_o^* \frac{d\delta_o^*}{dx} = \text{Constant}$, the following linear equation (reference 17):

$$g_1 \Delta + \frac{d\Delta}{d\xi} = g_2 u' + g_3 \frac{du'}{d\xi} + g_4 \frac{d^2 u'}{d\xi^2} - \frac{1}{g_1} \frac{d\Delta}{d\xi} \left(g_2 u' + 3g_3 \frac{du'}{d\xi} + 5g_4 \frac{d^2 u'}{d\xi^2} \right) \quad (7)$$

where

$$\xi = \frac{x}{\delta_o^*}$$

$$\left. \begin{aligned} g_1 &= \frac{1}{Re} \frac{(263)^2}{(37)(630)} \sigma^{-\frac{\gamma}{\gamma-1}} \left(1 - \frac{74}{263} \sigma \right)^2 \\ g_2 &= -g_1 \left[1 - \frac{2(\gamma-1)M_o^2}{\sigma} \left(\frac{1}{1 - \frac{74}{263} \sigma} + \frac{2-\gamma}{2(\gamma-1)} \right) \right] \\ g_3 &= \frac{(3-\gamma)M_o^2}{2\sigma} - 2 - \frac{\frac{15934}{9731} + \frac{74588}{360047} \frac{1}{\sigma}}{1 - \frac{74}{263} \sigma} \\ g_4 &= -Re \sigma^{\frac{1}{\gamma-1}} \frac{5}{888} \left(\frac{630}{263} \right)^3 \left(1 - \frac{74}{263} \sigma \right)^{-3} \end{aligned} \right\} \quad (8)$$

with

$$Re = \frac{U \delta_o^*}{\nu_o}$$

The momentum integral thus relates the displacement-thickness perturbation Δ to the velocity perturbation and its derivatives along the edge of the boundary layer.

SOLUTION OF BOUNDARY-VALUE PROBLEM OF OUTER FLOW

Until now the study has been directed at obtaining an explicit relationship for the boundary-layer displacement thickness as given in equation (7). Now the extent of the interaction zone is only a fraction of the distance from the leading edge of the plate, hence $\delta_0^*(x)$ can be assumed to be constant over this range. Equation (7) then becomes a linear equation with constant coefficients.

The problem is now one of determining the supersonic potential flow past a thin body whose thickness at any point corresponds to the perturbed boundary-layer thickness at that point. Consider the problem in the coordinates shown in figure 2.

The undisturbed thickness is seen to correspond to $y = 0$. Strictly speaking, the undisturbed thickness should be at $y = \delta_0^*$ in the physical plane. But since the outer flow does not depend upon the location of the origin of coordinates, the boundary conditions can be simplified slightly by choosing the axes as indicated in figure 2. Then, consistent with linear theory, the boundary conditions are satisfied at the undisturbed surface, namely, $y = 0$.

The linearized differential equation for the perturbation velocity potential of the supersonic stream is

$$m_\infty^2 \frac{\partial^2 \phi}{\partial \xi^2} - \frac{\partial^2 \phi}{\partial \eta^2} = 0 \quad (9)$$

where $\xi = \frac{x}{\delta_0^*}$ and $\eta = \frac{y}{\delta_0^*}$, and the general solution is given by

$$\phi = f(\xi - m_\infty \eta) + g(\xi + m_\infty \eta) \quad (10)$$

The incident waves will be taken as

$$\left. \begin{aligned} g(\xi + m_\infty \eta) &= 0 && \text{when } \xi + m_\infty \eta < 0 \\ g(\xi + m_\infty \eta) &= -\frac{\epsilon}{m_\infty}(\xi + m_\infty \eta) && \text{when } \xi + m_\infty \eta > 0 \end{aligned} \right\} \quad (11)$$

This corresponds to a simple compression wave, of deflection angle ϵ , incident upon the origin. (According to the above definition, the absolute value of ϵ will be used in any computations.)

Upstream Solution

The incident wave causes the boundary layer to be perturbed upstream and downstream of the point of incidence. Since no disturbances can be propagated upstream into the supersonic flow, the physically possible solutions in region 1 will be waves of the form $\phi_1 = f(\xi - m_\infty \eta)$. The normal velocity component at the boundary must be zero, hence the condition that the slope of the streamline is equal to the slope of the displacement boundary-layer thickness δ^* is imposed. The velocity vector of the supersonic flow has components $[U(1 + u'), Uv']$, where $u' = \partial\phi/\partial\xi$ and $v' = \partial\phi/\partial\eta$, so that the linearized boundary condition becomes

$$\frac{d\Delta}{d\xi} = \frac{\partial\phi}{\partial\eta} \quad \text{at } \eta = 0$$

or

$$\frac{d\Delta}{d\xi} = -m_\infty f'(\xi) \quad \text{at } \eta = 0 \quad (12)$$

Now since the boundary condition is on $d\Delta/d\xi$ rather than Δ , equation (7) is differentiated with respect to ξ , considering δ_0^* to be constant:

$$\begin{aligned}
g_1 \frac{d\Delta}{d\xi} + \frac{d^2\Delta}{d\xi^2} &= g_2 \frac{du'}{d\xi} + g_3 \frac{d^2u'}{d\xi^2} + g_4 \frac{d^3u'}{d\xi^3} - \\
&\quad \frac{1}{g_1} \frac{d^2\Delta}{d\xi^2} \left(g_2 u' + 3g_3 \frac{du'}{d\xi} + 5g_4 \frac{d^2u'}{d\xi^2} \right) - \\
&\quad \frac{1}{g_1} \frac{d\Delta}{d\xi} \left(g_2 \frac{du'}{d\xi} + 3g_3 \frac{d^2u'}{d\xi^2} + 5g_4 \frac{d^3u'}{d\xi^3} \right) \quad (13)
\end{aligned}$$

If the boundary condition (12) is substituted into equation (13), and it is noted that at $\eta = 0$, $\frac{du'}{d\xi} = f''(\xi)$, and so forth, an ordinary nonlinear differential equation for $f(\xi)$ will be obtained. By linearizing this equation:

$$g_4 f^{iv}(\xi) + g_3 f'''(\xi) + (g_2 + m_\infty) f''(\xi) + g_1 m_\infty f'(\xi) = 0 \quad (14)$$

The coefficients in equation (14) are constant for a specific case of Mach number and Reynolds number, hence the solution can be immediately written as

$$f(\xi) = A_0 + A e^{\lambda_2 \xi} + B_0 e^{\lambda_1 \xi} + C_0 e^{\lambda_3 \xi} \quad (15)$$

where the λ_n 's are roots of the equation

$$g_4 \lambda^3 + g_3 \lambda^2 + (g_2 + m_\infty) \lambda + g_1 m_\infty = 0 \quad (16)$$

For the cases under consideration equation (16) has three real roots, one positive and two negative. Let $\lambda_2 > 0$, $\lambda_1 < 0$, and $\lambda_3 < 0$. In order to have all disturbances vanish as $\xi \rightarrow -\infty$ it is seen from equation (15) that

$$B_0 = C_0 = A_0 = 0$$

The upstream solution is then

$$f(\xi - m_\infty \eta) = Ae^{\lambda_2(\xi - m_\infty \eta)} \quad (17)$$

or in the physical plane

$$\left. \begin{aligned} \phi_1 &= Ae^{\frac{\lambda_2}{\delta_0^*}(x - m_\infty y)} \\ x - m_\infty y &< 0 \end{aligned} \right\} \quad (18)$$

The solution in region 2 follows immediately. The equation for the outer flow is linear, hence, by adding solutions,

$$\left. \begin{aligned} \phi_2 &= Ae^{\frac{\lambda_2}{\delta_0^*}(x - m_\infty y)} - \frac{\epsilon}{m_\infty} \frac{1}{\delta_0^*}(x + m_\infty y) \\ x - m_\infty y &< 0 \\ x + m_\infty y &> 0 \end{aligned} \right\} \quad (19)$$

Downstream Solution

In region 3 the solution to the linearized supersonic flow equation is

$$\phi_3 = g(\xi + m_\infty \eta) + h(\xi - m_\infty \eta)$$

But $g(\xi + m_\infty \eta)$ is known since it is the incident wave, hence use of the boundary condition at the interface will result in an ordinary differential equation for $h(\xi)$. The nondimensionalized boundary condition takes the form

$$\frac{d\Delta}{d\xi} = -m_\infty h'(\xi) - \epsilon \quad \text{at } \eta = 0 \quad (20)$$

since
$$\frac{\partial \phi}{\partial \eta} = -\epsilon - m_\infty h'(\xi)$$

Substituting equation (20) into equation (13),

$$g_4 h^{iv} + g_3 h''' + (g_2 + m_\infty) h'' + g_1 m_\infty h' = -g_1 \epsilon \quad (21)$$

It can be seen that the complementary solution will be identical to equation (15). Hence the complete solution is

$$h(\xi) = D_0 + E e^{\lambda_2 \xi} + B e^{\lambda_1 \xi} + C e^{\lambda_3 \xi} - \frac{\epsilon}{m_\infty} \xi \quad (22)$$

where again $\lambda_2 > 0$, $\lambda_1 < 0$, and $\lambda_3 < 0$. Choose $D_0 = 0$ without affecting any of the physical quantities such as velocity or pressure since $h(\xi)$ merely represents a velocity potential. To eliminate the possibility of any velocity becoming infinite as $\xi \rightarrow \infty$ put $E = 0$. Then the solution becomes

$$\left. \begin{aligned} h(\xi) &= B e^{\lambda_1 \xi} + C e^{\lambda_3 \xi} - \frac{\epsilon}{m_\infty} \xi \\ h(\xi - m_\infty \eta) &= B e^{\lambda_1 (\xi - m_\infty \eta)} + C e^{\lambda_3 (\xi - m_\infty \eta)} - \frac{\epsilon}{m_\infty} (\xi - m_\infty \eta) \end{aligned} \right\} \quad (23)$$

Then the perturbed velocity potential in region 3 is

$$\left. \begin{aligned} \phi_3 &= B e^{\frac{\lambda_1}{\delta_0^*} (x - m_\infty y)} + C e^{\frac{\lambda_3}{\delta_0^*} (x - m_\infty y)} - \frac{2\epsilon}{m_\infty} \frac{x}{\delta_0^*} \\ x - m_\infty y &> 0 \end{aligned} \right\} \quad (24)$$

Determination of Constants

The problem now involves four constants A , B , C , and D^1 with three parameters M_∞ , ϵ , and Re . Additional conditions must therefore be imposed in order to determine the constants as functions of the

¹The constant D is a measure of the downstream boundary-layer thickness as shown in the following discussion.

parameters. It is noted that the outer flow field was divided into distinct regions by the lines OS and OM (figure 2), so that the boundary layers in regions 1 and 3 were treated independently of each other. These boundary layers are therefore related at the point of incidence by the following conditions:

(a) The boundary-layer displacement thickness must be continuous at $x = 0$

(b) The wall pressure must be continuous at $x = 0$

(c) Discontinuities, if any, must satisfy $\lim_{x_0 \rightarrow 0} \int_{-x_0}^{x_0} K dx = 0$

where $K = 0$ denotes the Kármán momentum equation for compressible viscous fluids

Condition (a).— Compute the boundary layers for regions 1 and 3 and then match the displacement thicknesses at the origin. One has as a boundary condition

$$\frac{d \Delta_1}{d \xi} = \frac{\partial \phi_1}{\partial \eta} \quad \text{at } \eta = 0, \quad i = 1 \text{ or } 3$$

where $\Delta_1 = \frac{\delta_1^*}{\delta_0^*} - 1$ and δ_1^* is the total boundary-layer displacement thickness in regions 1 or 3.

From equation (18) one obtains for region 1

$$\frac{d \Delta_1}{d \xi} = -m_\infty \lambda_2 A e^{\lambda_2 \xi}$$

$$\Delta_1 = -m_\infty A e^{\lambda_2 \xi} + \text{Constant}$$

All disturbances vanish far upstream so that $\Delta_1(-\infty) = 0$. But since $\lambda_2 > 0$, the exponential term vanishes as $\xi \rightarrow -\infty$, hence the constant equals zero. Therefore

$$\Delta_1 = -m_\infty A e^{\lambda_2 \xi}$$

or

$$\delta_1^* = \delta_0^* \left(1 - m_\infty A e^{\lambda_2 \frac{x}{\delta_0^*}} \right)$$

For region 3 one obtains, according to equations (24),

$$\frac{d \Delta_3}{d \xi} = -m_\infty B \lambda_1 e^{\lambda_1 \xi} - m_\infty C \lambda_3 e^{\lambda_3 \xi}$$

$$\Delta_3 = -m_\infty B e^{\lambda_1 \xi} - m_\infty C e^{\lambda_3 \xi} + \text{Constant}$$

Let $\Delta_3(\infty) = D$ and since the exponentials vanish at positive infinity, the constant equals D .
Therefore

$$\Delta_3 = -m_\infty B e^{\lambda_1 \xi} - m_\infty C e^{\lambda_3 \xi} + D$$

or

$$\delta_3^* = \delta_0^* \left(1 - m_\infty B e^{\lambda_1 \frac{x}{\delta_0^*}} - m_\infty C e^{\lambda_3 \frac{x}{\delta_0^*}} + D \right)$$

Thus it is seen that for the total downstream thickness

$$\lim_{\xi \rightarrow \infty} \delta_3^* = \delta_0^* (1 + D)$$

By putting $\delta_1^* = \delta_3^*$ at $x = 0$,

$$A = B + C - \frac{D}{m_\infty} \quad (25)$$

Condition (b).— Since the validity of the usual boundary-layer assumptions in the interaction zone has been assumed in the case of weak shock interaction, the pressure at the wall, as a first approximation, equals the pressure at the interface. The pressure at the wall as well as at the interface is therefore required to be continuous. As a consequence, the pressure jump due to the incident wave must necessarily be neutralized by a reflected expansion wave. This deduction is actually confirmed by experiments.

The pressure in each region consists of an undisturbed pressure p_0 plus a perturbed pressure p' due to the incident wave; $p = p_0 + p'$. Since the undisturbed pressure is the same throughout the flow field, only the perturbed pressures, which, by small perturbation theory,

are $p' = -\rho_\infty U u'$, will be considered. The velocity potentials ϕ_1 , ϕ_2 , and ϕ_3 have previously been found, and, accordingly, the pressures are given by

$$p_1' = -\gamma M_\infty^2 p_0 A \lambda_2 e^{\frac{\lambda_2}{\delta_0^*}(x-m_\infty y)} \quad (26)$$

$$p_3' = -\gamma M_\infty^2 p_0 \left[B \lambda_1 e^{\frac{\lambda_1}{\delta_0^*}(x-m_\infty y)} + C \lambda_3 e^{\frac{\lambda_3}{\delta_0^*}(x-m_\infty y)} - \frac{2\epsilon}{m_\infty} \right] \quad (27)$$

The condition for continuous pressure at the origin is

$$p_1' = p_3'$$

hence

$$A \lambda_2 = B \lambda_1 + C \lambda_3 - \frac{2\epsilon}{m_\infty} \quad (28)$$

This condition shows that the discontinuity between regions 2 and 3 corresponds, in linear theory, to an expansion of the flow from regions 2 to 3 by a wave of the same magnitude as the incident wave. Now since λ_1 and λ_3 are negative, the downstream pressure along the interface $y = 0$ is

$$p_3' \rightarrow \frac{\gamma M_\infty^2}{m_\infty} p_0 (2\epsilon) \quad (29)$$

as $\xi \rightarrow \infty$. This asymptotic value of the pressure is exactly twice the incident pressure rise; therefore, as anticipated, the incident wave is reflected as a regular reflection from a solid boundary.

Condition (c).—The Kármán momentum-integral equation for compressible fluids is

$$\frac{d}{dx} \int_0^\delta \rho u^2 dy - u_e \frac{d}{dx} \int_0^\delta \rho u dy = -\frac{dp}{dx} \delta - \tau_w$$

where τ_w indicates the wall shear stress. With the ordinary definitions of the displacement and momentum thicknesses, the equation becomes

$$\frac{d}{dx}(\rho_e u_e^2 \theta) + \rho_e u_e \delta^* \frac{du_e}{dx} = \tau_w$$

From the outer flow

$$\rho_e u_e \frac{du_e}{dx} = - \frac{dp}{dx}$$

thus

$$\frac{d}{dx}(\rho_e u_e^2 \theta) - \delta^* \frac{dp}{dx} - \tau_w = 0$$

From the previous notation it is seen that

$$K \equiv \frac{d}{dx}(\rho_e u_e^2 \theta - \delta^* p) + p \frac{d\delta^*}{dx} - \tau_w$$

As the boundary-layer regions 1 and 3 are independently considered, the pressure gradient and velocity therein might be discontinuous at the origin. In order that the discontinuities be consistent with the dynamical equations, it is necessary that:

$$\lim_{x_0 \rightarrow 0} \int_{-x_0}^{x_0} \left[\frac{d}{dx}(\rho_e u_e^2 \theta - \delta^* p) + p \frac{d\delta^*}{dx} - \tau_w \right] dx = 0$$

or

$$\lim_{x_0 \rightarrow 0} \left[\left(\rho_e u_e^2 \theta - \delta^* p \right)_{-x_0}^{x_0} + \int_{-x_0}^{x_0} p \frac{d\delta^*}{dx} dx - \int_{-x_0}^{x_0} \tau_w dx \right] = 0$$

Now δ^* is required to be continuous at the origin, $p \frac{d\delta^*}{dx}$, discontinuous but finite, and the shear stress τ_w , finite; then, in the limit, the

two integrals vanish and

$$\lim_{x_0 \rightarrow 0} \left(\rho_e u_e^{2\theta} - \delta^* p \right)_{-x_0}^{x_0} = 0$$

remains. Therefore, in the limit,

$$\rho_3 u_3^{2\theta_3} - \rho_1 u_1^{2\theta_1} - \delta^*(0)(p_3 - p_1) = 0 \quad (30)$$

The condition that $p_1 = p_3$ at $x = y = 0$ has already been imposed and hence equation (30) reduces to

$$\rho_1 u_1^{2\theta_1} = \rho_3 u_3^{2\theta_3} \quad \text{at } x = y = 0 \quad (31)$$

This equation, linearized in u' and its derivatives, becomes

$$\alpha_1 \delta_o^* \left(\frac{du_3'}{dx} - \frac{du_1'}{dx} \right) = \alpha_2 (u_3' - u_1') \quad (32)$$

where

$$\alpha_1 \equiv - \frac{\text{Re}}{\left(\frac{37}{315} - \frac{263}{630\sigma} \right)^3} \sigma^{\frac{3(2-\gamma)}{2(\gamma-1)}} \left\{ \frac{1}{111\sigma} + \frac{\left[\frac{1}{3} \left(\frac{71}{2520} \right) \sigma^{-2} - \frac{\sigma^{-1}}{945} \right]}{\left(\frac{37}{315} - \frac{263}{630\sigma} \right)} \right\}$$

$$\alpha_2 \equiv -\sigma^{\frac{2-\gamma}{2(\gamma-1)}} \left(\frac{37}{315} - \frac{263}{630\sigma} \right)^{-1} \left[2 + M_\infty^2 \left(\frac{263}{630} \frac{\gamma-1}{\sigma} - 1 \right) \right]$$

The pressures were equal at the origin, so that, in linear theory, the streamwise perturbation velocities are also equal. Therefore $u_1' = u_3'$ at $x = y = 0$.

Now since $\alpha_1 \neq 0$ and $\alpha_2 \neq 0$, for the range of M_∞ and Re studied

$$\frac{du_1'}{dx} = \frac{du_3'}{dx} \quad \text{at } x = y = 0 \quad (33)$$

It is therefore seen that, in the linear theory, continuous pressure also implies continuous pressure gradient. Since

$$\frac{du_1'}{dx} = \frac{A\lambda_2^2}{\delta_0^*} \quad \text{at } x = y = 0$$

$$\frac{du_3'}{dx} = \frac{1}{\delta_0^*} (B\lambda_1^2 + C\lambda_3^2) \quad \text{at } x = y = 0$$

there is obtained from equation (33)

$$A\lambda_2^2 = B\lambda_1^2 + C\lambda_3^2 \quad (34)$$

Conditions (a), (b), and (c) lead to equations (25), (28), and (34) for four constants A, B, C, and D. But previously it has been shown that

$$\lim_{\xi \rightarrow \infty} \delta_3^* = \delta_0^*(1 + D)$$

Thus it is seen that D merely determines the downstream boundary-layer thickness, whereas A, B, and C determine the local character of the perturbation. Therefore, if the downstream thickness can be estimated, there will be a determinate problem. Assume for the present at least, that D is determined. The constants A, B, and C can then be solved for from the following equations:

$$A\lambda_2 = B\lambda_1 + C\lambda_3 - \frac{2\epsilon}{m_\infty}$$

$$A = B + C - \frac{D}{m_\infty}$$

$$A\lambda_2^2 = B\lambda_1^2 + C\lambda_3^2$$

The solution is

$$\left. \begin{aligned} A &= \frac{-(\lambda_3 + \lambda_1)}{(\lambda_2 - \lambda_3)(\lambda_2 - \lambda_1)} \left(-\frac{2\epsilon}{m_\infty}\right) + \frac{\lambda_1 \lambda_3}{(\lambda_2 - \lambda_3)(\lambda_2 - \lambda_1)} \left(-\frac{D}{m_\infty}\right) \\ B &= \frac{(\lambda_3 + \lambda_2)}{(\lambda_3 - \lambda_1)(\lambda_2 - \lambda_1)} \left(-\frac{2\epsilon}{m_\infty}\right) - \frac{\lambda_2 \lambda_3}{(\lambda_3 - \lambda_1)(\lambda_2 - \lambda_1)} \left(-\frac{D}{m_\infty}\right) \\ C &= \frac{-(\lambda_2 + \lambda_1)}{(\lambda_3 - \lambda_1)(\lambda_2 - \lambda_3)} \left(-\frac{2\epsilon}{m_\infty}\right) + \frac{\lambda_1 \lambda_2}{(\lambda_3 - \lambda_1)(\lambda_2 - \lambda_3)} \left(-\frac{D}{m_\infty}\right) \end{aligned} \right\} \quad (35)$$

Evaluation of D.— It is seen from equations (35) that the local perturbations are determined once the constant D is specified. As it has been shown that D characterizes the thickening of the boundary layer through a shock, it can be determined approximately by the following consideration.

When a weak shock is incident upon the boundary layer, it is assumed that the Kármán momentum-integral equation

$$\frac{d\theta}{dx} + \theta \left[\frac{1}{\rho_e} \frac{d\rho_e}{dx} + \left(2 + \frac{\delta^*}{\theta} \right) \frac{1}{u_e} \frac{du_e}{dx} \right] = \frac{\tau_w}{\rho_e u_e^2}$$

is valid throughout the disturbed boundary-layer flow. For a given pressure distribution, the growth of the boundary layer is governed by this equation. When a shock is incident upon the boundary layer, it has been theoretically predicted and experimentally verified that the flow upstream of the point of incidence is separated over a considerable portion of the disturbed flow; hence the shear stress becomes relatively unimportant. Downstream of the point of incidence, since the flow is dominated by pressure forces, whether the flow is laminar or turbulent the shear is known, from experimental results, to be very small (reference 18). Hence for the present approximation, the shear stress can be neglected.

Furthermore, if the ratio $\delta^*/\theta \equiv H$ is regarded as a parameter, the momentum equation gives the momentum thickness as a function of $u_e(x)$. Now, it is known that H is substantially increased by the shock, and to a lesser extent by the compressibility. In going through a shock, H first increases because of the shock and then decreases because of the drop in Mach number. Hence, as a first approximation, H can be taken to be some constant average value over the interaction range. (This is

similar to the procedure mentioned by Nitzberg and Crandall (reference 19).) In particular, H will be taken as the value ahead of the interaction.

The momentum-integral equation now becomes:

$$\frac{1}{\theta} \frac{d\theta}{dx} + \frac{1}{\rho_e} \frac{d\rho_e}{dx} + (2 + H) \frac{1}{u_e} \frac{du_e}{dx} = 0$$

or

$$\frac{d}{dx} \left(\log_e \theta \rho_e u_e^{2+H} \right) = 0$$

Integrating between regions 1 and 3, stations far upstream and downstream of the point of incidence,

$$\theta_1 \rho_1 u_1^{2+H} = \theta_3 \rho_3 u_3^{2+H}$$

or

$$\frac{\delta_3^*}{\delta_1^*} = \frac{\rho_1}{\rho_3} \left(\frac{u_1}{u_3} \right)^{2+H} \quad (36)$$

For laminar flow over a flat plate where $\mu \propto T$, $Pr = 1$, and $(\partial T / \partial y)_w = 0$, the formula given by Lees (reference 20, p. 119) for H can be taken:

$$H = 2.50 + 3.50 \left(\frac{\gamma - 1}{2} \right) M_\infty^2$$

The thickening predicted by equation (36) is shown in figure 3. Values of the density and velocity ratios were computed exactly and to first order in the deflection angle. For small deflection angles, the agreement between the "exact" thickness ratio and that obtained from linear theory is quite good. The crosses on figure 3 are the experimental values for various Reynolds numbers obtained by Barry, Shapiro, and Neumann (reference 4), and there is fair agreement between theory and experiment. Actually, the experimental data are visual estimates of the ratio of boundary-layer thicknesses, so that for a comparison between

theory and experiment, the ratio of boundary-layer thickness to displacement thickness would have to be assumed to be the same upstream as well as downstream of the point of incidence. In view of the assumption and the allowable experimental error in the visualization of schlieren photographs, the experimental values must be regarded as qualitative. The theoretical values of the thickness ratio are near the lower limit of the experimental values. This is probably due to the fact that the value of H was underestimated, since an average H through the interaction range would be larger than the initial value.

Evaluating D according to the linear theory,

$$\frac{\delta_3^*}{\delta_1^*} = \frac{\rho_1}{\rho_3} \left(\frac{u_1}{u_3} \right)^{2+H}$$

and

$$\frac{\rho_1}{\rho_3} = 1 - \frac{2M_\infty^2}{m_\infty} \epsilon$$

$$\frac{u_1}{u_3} = 1 + \frac{2\epsilon}{m_\infty}$$

hence

$$\frac{\rho_1}{\rho_3} \left(\frac{u_1}{u_3} \right)^{2+H} = 1 + \left(2 + H - M_\infty^2 \right) \frac{2\epsilon}{m_\infty}$$

But

$$\frac{\delta_3^*}{\delta_1^*} = 1 + D$$

Therefore

$$D = \frac{2\epsilon}{m_\infty} \left(2 + H - M_\infty^2 \right)$$

Now since

$$H = 2.50 + 3.50 \left(\frac{\gamma - 1}{2} \right) M_\infty^2$$

$$D = \frac{2\epsilon}{m_\infty} (4.50 - 0.3M_\infty^2) \quad (37)$$

Effects of Downstream Thickening

Consider the constant A governing the upstream flow:

$$A = \frac{-(\lambda_3 + \lambda_1)}{(\lambda_2 - \lambda_3)(\lambda_2 - \lambda_1)} \left(-\frac{2\epsilon}{m_\infty} \right) + \frac{\lambda_1 \lambda_3}{(\lambda_2 - \lambda_3)(\lambda_2 - \lambda_1)} \left(-\frac{D}{m_\infty} \right)$$

or

$$A = -\frac{2\epsilon}{m_\infty} \left[\frac{-(\lambda_3 + \lambda_1)}{(\lambda_2 - \lambda_3)(\lambda_2 - \lambda_1)} + \frac{\lambda_1 \lambda_3}{(\lambda_2 - \lambda_3)(\lambda_2 - \lambda_1)} \left(\frac{4.50 - 0.3M_\infty^2}{m_\infty} \right) \right]$$

The coefficients are given in table I; hence it is seen that for all cases in the present range of Mach numbers and Reynolds numbers the contribution of D toward A amounts to less than 10 percent. Thus it is seen that, in the present range, a precise knowledge of the downstream thickness is not essential to the determination of the upstream flow.

The effect on the downstream flow is not quite so straightforward, since two constants B and C are involved. As an indication of the downstream flow, consider the pressure distribution along the wall. It has been seen that, far downstream, the pressure attains a constant value, namely the pressure that would have been anticipated had there been a regular reflection. Immediately behind the point of incidence the pressure is much lower than this end pressure since the flow has just undergone an expansion to the pressure that existed before the point of incidence. The manner in which the pressure proceeds from its value at the origin to its final downstream value is then of some importance. Does the pressure increase monotonically to its final value, or does the pressure at any point rise higher than the final value? Liepmann (reference 3) has found experimentally that for the reflection of a shock wave from a laminar boundary layer there indeed exists a definite downstream overcompression. The pressure rises sharply to some value higher than

the end pressure and then tapers off. The experimental findings of Barry, Shapiro, and Neumann (reference 4) also confirm this observation, although their results show the overcompression to be slightly less pronounced.

Consider the behavior of the theoretical downstream pressure distribution. Along the interface the total pressure is given as

$$p_3 = p_0 - \gamma M_\infty^2 p_0 \left(B \lambda_1 e^{\lambda_1 \frac{x}{\delta_0^*}} + C \lambda_3 e^{\lambda_3 \frac{x}{\delta_0^*}} - \frac{2\epsilon}{m_\infty} \right) \quad (38)$$

and

$$p_3 \longrightarrow p_0 \left(1 + \frac{2\gamma M_\infty^2}{m_\infty} \epsilon \right) \quad (39)$$

as

$$\frac{x}{\delta_0^*} = \xi \longrightarrow \infty$$

so that far downstream, consistent with linear theory, the correct pressure behind the regular reflection is obtained. Then

$$B = \frac{(\lambda_3 + \lambda_2)}{(\lambda_3 - \lambda_1)(\lambda_2 - \lambda_1)} \left(-\frac{2\epsilon}{m_\infty} \right) + \frac{\lambda_2 \lambda_3}{(\lambda_3 - \lambda_1)(\lambda_2 - \lambda_1)} \left(\frac{D}{m_\infty} \right)$$

wherein $\epsilon > 0$ and $D > 0$. Now $\lambda_2 > 0$, $\lambda_1 < 0$, and $\lambda_3 < 0$, where λ_2 and λ_1 are of the same order of magnitude, while λ_3 is about ten times as small. Hence $B < 0$.

Consider

$$C = \frac{-(\lambda_2 + \lambda_1)}{(\lambda_3 - \lambda_1)(\lambda_2 - \lambda_3)} \left(-\frac{2\epsilon}{m_\infty} \right) + \frac{\lambda_1 \lambda_2}{(\lambda_3 - \lambda_1)(\lambda_2 - \lambda_3)} \left(-\frac{D}{m_\infty} \right)$$

$$C = \frac{2\epsilon}{m_\infty} \left[\frac{(\lambda_2 + \lambda_1)}{(\lambda_3 - \lambda_1)(\lambda_2 - \lambda_3)} - \frac{\lambda_1 \lambda_2}{(\lambda_3 - \lambda_1)(\lambda_2 - \lambda_3)} \left(\frac{4.50 - 0.3M_\infty^2}{m_\infty} \right) \right]$$

Now the second term is always negative in the Mach number range considered, whereas the first term may be either positive or negative depending upon the sign of $\lambda_2 + \lambda_1$. It turns out that for $M_\infty > 2.4$ (approx.) the first term is positive, hence $C > 0$. For $M_\infty < 2.4$ (approx.) the first term is negative, but

$$\left| \frac{(\lambda_2 + \lambda_1)}{(\lambda_3 - \lambda_1)(\lambda_2 - \lambda_3)} \right| < \left| \frac{\lambda_1 \lambda_2}{(\lambda_3 - \lambda_1)(\lambda_2 - \lambda_3)} \left(\frac{4.50 - 0.3M_\infty^2}{m_\infty} \right) \right|$$

hence C is positive. Thus for the whole range of Mach numbers and Reynolds numbers, $C > 0$.

The qualitative behavior of the downstream pressure distribution will now be established. The downstream pressure along the interface is

$$p_3 = p_0 + \gamma M_\infty^2 p_0 \frac{2\epsilon}{m_\infty} + \gamma M_\infty^2 p_0 \left(-B\lambda_1 e^{\lambda_1 \frac{x}{\delta_{0*}}} - C\lambda_3 e^{\lambda_3 \frac{x}{\delta_{0*}}} \right)$$

The first two terms represent the constant end pressure while the third actually describes the variation of the pressure. Consider the curve

$$y = -B\lambda_1 e^{\lambda_1 \frac{x}{\delta_{0*}}} - C\lambda_3 e^{\lambda_3 \frac{x}{\delta_{0*}}}$$

It is known that $B < 0$, $C > 0$, $\lambda_1 < 0$, and $\lambda_3 < 0$; hence $-B\lambda_1 < 0$ and $-C\lambda_3 > 0$. The constants B and C are of the same order of magnitude, but λ_1 is about ten times as large as λ_3 ; hence

$$|B\lambda_1| > |C\lambda_3|$$

Therefore, when $x = 0$, y is negative and, when x becomes large, y is positive but small. The point at which the maximum occurs is given by

$$\left(\frac{x}{\delta_{0*}} \right)_{y_{\max}} = \frac{1}{\lambda_3 - \lambda_1} \log_e \left(-\frac{B\lambda_1^2}{C\lambda_3^2} \right)$$

If

$$y = -B\lambda_1 e^{\lambda_1 \frac{x}{\delta_o^*}} - C\lambda_3 e^{\lambda_3 \frac{x}{\delta_o^*}}$$

is now interpreted as the pressure variation, it is immediately seen that the theoretical pressure distribution exhibits the overcompression that is observed experimentally.

RESULTS AND DISCUSSION

It has been seen that if the downstream thickening is estimated, the constants A, B, and C are completely determined as functions of the flow parameters. With the outer flow thus determined, the boundary-layer growth and pressure distributions can now be computed, and hence the effects of Mach number, Reynolds number, and shock strength upon the upstream influence and the location of the separation point can be studied. (Of course, when the results are compared with experiment, the Reynolds numbers must be low enough so that the boundary layer will remain laminar, prior to the interaction, in the corresponding experimental case.)

Upstream Influence

In order to estimate the upstream influence of the interaction, define a length in which the pressure on the boundary-layer displacement thickness decays to a specified fraction of its amplitude at the origin. This length would then be determined solely by the exponent λ_2 . For example, consider the upstream boundary-layer disturbance:

$$\delta_1^* = -m_\infty A \delta_o^* e^{\lambda_2 \frac{x}{\delta_o^*}}$$

At the origin

$$\delta_1^*(0) = -m_\infty A \delta_o^*$$

If x_d/δ_o^* is defined as the distance required in order that $\delta_1^* = \alpha(-m_\infty A \delta_o^*)$ at x_d/δ_o^* where $\alpha < 1$,

$$\alpha(-m_\infty A \delta_o^*) = -m_\infty A \delta_o^* e^{\lambda \frac{x}{2\delta_o^*}}$$

Therefore

$$\frac{x_d}{\delta_o^*} = -\frac{1}{\lambda_2} \log_e \left(\frac{1}{\alpha} \right)$$

Since α is a constant it is seen that the upstream influence is then inversely proportional to λ_2 . Values of λ_2 have been plotted in figure 4. (Values of λ_1 and λ_3 are plotted in figures 5 and 6, respectively.) For fixed Mach number, x_d/δ_o^* increases with increasing Reynolds number. For large Reynolds number, this dependence can be deduced from the equation:

$$\lambda^3 + \frac{g_3}{g_4} \lambda^2 + \left(\frac{g_2}{g_4} + \frac{m_\infty}{g_4} \right) \lambda + \frac{m_\infty g_1}{g_4} = 0$$

The coefficients are functions of Mach number and for the range of Mach numbers considered, the roots are real. When the Reynolds number is large, it can be shown that

$$\lambda_2 \approx \frac{\sqrt{m_\infty}}{\sqrt{-g_4}}$$

where $g_4(\text{Re}, M_\infty) < 0$ and $g_4 \propto \text{Re}$. This is in agreement with Lees' result. Consequently, for large Reynolds numbers, $x_d/\delta_o^* \propto \text{Re}^{1/2}$. For fixed Reynolds numbers, the upstream influence decreases with increasing Mach number as indicated in figure 4(b). If the disturbance is considered to decay to, say, 5 percent of its amplitude at the origin, it is found that, at the high Reynolds numbers, and Mach numbers about 2 or less, the upstream influence is of the order of 30 boundary-layer displacement thicknesses.

The result that the upstream influence increases with Reynolds number may appear to be disconcerting since the viscous effects are expected to be more prevalent at the lower Reynolds numbers and hence to produce a greater influence upon the upstream flow. This apparent paradox arises because the upstream influence has been measured in multiples of a length which is also dependent upon Reynolds number. If the absolute values of upstream influence are considered,

$$\frac{x_d}{\delta_o^*} \propto Re^{1/2}$$

But

$$\delta_o^* \propto \frac{1}{Re_x^{1/2}} \propto \frac{1}{Re}$$

hence

$$x_d \propto \delta_o^* Re^{1/2}$$

or

$$x_d \propto Re^{-1/2}$$

Thus, measured on an absolute scale, the upstream influence increases with decreasing Reynolds number.

As defined above, the distance of the upstream influence is dependent solely upon Mach number and Reynolds number. It can be redefined so that it will also depend upon the shock strength. This is accomplished by defining the upstream influence to be that distance at which the disturbance decays to a given fraction of the undisturbed value. The perturbed boundary-layer displacement thickness ahead of the point of incidence is given by:

$$\delta_1^* = -m_\infty A \delta_o^* e^{\lambda \frac{x}{2\delta_o^*}}$$

where δ_o^* is the undisturbed displacement thickness. The upstream

influence is then the distance x_d/δ_o^* to the point where $\delta_1^* = b\delta_o^*$ and $b < 1$:

$$b\delta_o^* = -m_\infty A \delta_o^* e^{\lambda_2 \frac{x}{2\delta_o^*}}$$

$$\lambda_2 \frac{x_d}{\delta_o^*} = \log_e \left(-\frac{b}{m_\infty A} \right)$$

$$\frac{x_d}{\delta_o^*} = -\frac{1}{\lambda_2} \log_e \left(-\frac{m_\infty A}{b} \right)$$

Now A is negative and decreases with increase of the deflection angle, so that for fixed Mach number and Reynolds number, the upstream influence decreases with shock strength. If the upstream influence is measured to the point at which the disturbance decays to 5 percent of its undisturbed value, $b = 0.05$. In figure 7, x_d/δ_o^* is plotted against deflection angle. For $\epsilon \leq 2^\circ$, the results seem to agree fairly well with the experimental values presented in figure 10, reference 2. For larger deflection angles, however, the theoretical values are too low in comparison with the experimental values. This might be due to the fact that the linear theory becomes less accurate as the deflection angle increases.

Boundary-Layer Separation

Since the outer potential flow is known, the point of separation can be computed on the basis that separation occurs when $(\partial u/\partial y)_w = 0$. Now $\partial u/\partial y$ is proportional to $\partial u/\partial y'$ so that one can just as well use $(\partial u/\partial y')_w = 0$ as a criterion for separation. In view of the assumption of a Pohlhausen velocity profile, in the transformed plane

$$\left(\frac{\partial u}{\partial y'} \right)_w = \frac{u_e}{\delta'} \left(2 + \frac{\Lambda}{6} \right)$$

hence, as in the incompressible case, separation occurs at $\Lambda = -12$. Now it is known from experience in the incompressible case that, in regions of retarded flow, the Kármán-Pohlhausen method gives values of the skin friction that are too high and consequently predicts separation too late or not at all. This feature of the method is also to be

expected in the compressible case, since it was shown by Howarth that the effect of compressibility is equivalent to exaggerating the pressure gradient in the incompressible case (reference 13). In particular, Stewartson has used the Kármán-Pohlhausen method to treat the case of flow against a linear pressure gradient and has shown that the predicted distance from the leading edge to the separation point is an overestimate of the actual value (reference 21).

In the present problem, where the flow upstream of the point of incidence is subject to a positive pressure gradient, the same overestimation of the separation point will, of course, be expected. But the effects of Mach number, Reynolds number, and shock strength upon the separation point are of primary interest, so that inaccuracy in the absolute values is unimportant.

It is known from the boundary-layer theory that the parameter that defines the separation point is

$$\Lambda = \frac{(\delta')^2}{v_o} \frac{du_e}{dx} \left(1 + \frac{\gamma - 1}{2} M_e^2 \right)$$

By neglecting products of u' and its derivatives,

$$\Lambda = \left[(\delta')^2 / v_o \right] (U/\sigma) (du'/dx)$$

Now, from equation (6), to the order of approximation,

$$\Lambda = \frac{\text{Re } \delta_o^*}{\left(\frac{37}{315} - \frac{263}{630\sigma} \right)^2} \sigma^{\frac{3-2\gamma}{\gamma-1}} \frac{du'}{dx}$$

Along the edge of the boundary layer, from the upstream solution (see equation (18))

$$\frac{du'}{dx} = A \frac{\lambda_2^2}{\delta_o^*} e^{\lambda_2 \frac{x}{2\delta_o^*}}$$

so that

$$\Lambda = \frac{A \operatorname{Re} \lambda_2^2}{\left(\frac{37}{315} - \frac{263}{630\sigma}\right)^2} \sigma^{\frac{3-2\gamma}{\gamma-1}} e^{\lambda_2 \frac{x}{2\delta_0^*}}$$

For separation

$$\begin{aligned} -12 &= \frac{A \operatorname{Re} \lambda_2^2}{\left(\frac{37}{315} - \frac{263}{630\sigma}\right)^2} \sigma^{\frac{3-2\gamma}{\gamma-1}} e^{\lambda_2 \frac{x_B}{2\delta_0^*}} \\ \frac{x_B}{\delta_0^*} &= -\frac{1}{\lambda_2} \log_e \left(\frac{A \operatorname{Re} \lambda_2^2}{-12} \beta \right) \end{aligned} \quad (40)$$

where

$$\beta \equiv \frac{\sigma^{\frac{3-2\gamma}{\gamma-1}}}{\left(\frac{37}{315} - \frac{263}{630\sigma}\right)^2}$$

and λ_2 is positive, hence separation ahead of the point of incidence will be predicted only when $-\frac{1}{12} A \operatorname{Re} \lambda_2^2 \beta > 1$.

Contrary to the separation phenomenon in ordinary boundary-layer flow, the location of the separation point is influenced by the Reynolds number. This is easily understood when one considers the fact that separation of the flow is controlled by the pressure gradient of the outer flow; according to boundary-layer theory, the outer flow depends solely upon the geometry of the body. Consequently, the location of the separation point is independent of Reynolds number. In the present problem, however, an outer flow that is compatible with the boundary-layer flow has to be found. This relationship is expressed by the condition which requires that the direction of the potential flow be the same as the slope of the displacement thickness. Since the boundary-layer growth depends upon the Reynolds number, the outer flow, and eventually the separation point, must also vary with Reynolds number.

In order to determine the effect of shock strength upon the position of the separation point, the constant A must be examined:

$$A = -\frac{2\epsilon}{m_\infty} \left[\frac{-(\lambda_3 + \lambda_1)}{(\lambda_2 - \lambda_3)(\lambda_2 - \lambda_1)} + \frac{\lambda_1 \lambda_3}{(\lambda_2 - \lambda_3)(\lambda_2 - \lambda_1)} \left(\frac{4.50 - 0.3M_\infty^2}{m_\infty} \right) \right]$$

For the range of Mach numbers and Reynolds numbers considered, the terms in the bracket are positive, since $\lambda_2 > 0$, $\lambda_1 < 0$, and $\lambda_3 < 0$. Therefore as ϵ is increased A becomes more negative; consequently $-\frac{1}{12} A \text{Re } \lambda_2^2 \beta$ becomes more positive and hence the separation point moves upstream. Thus an increase of shock strength increases the distance between the separation point and the point of incidence.

To express x_s/δ_o^* explicitly in terms of Mach number and Reynolds number would be difficult; hence this relationship will be presented numerically by varying, separately, the Mach number and Reynolds number. In figure 8, lines of constant Reynolds number are plotted in the $x_s/\delta_o^*, \epsilon$ plane, and the separation point, measured in multiples of δ_o^* , moves upstream with increasing Reynolds number. This is not too surprising since the same behavior occurs with the upstream influence. As the upstream influence increases, the "self-induced" pressure gradient will begin farther upstream and hence separation will occur farther upstream. For fixed Reynolds number, the upstream influence increased with decreasing Mach number, and accordingly (see fig. 9) the separation point, measured in multiples of δ_o^* , moves upstream with decreasing Mach number.

Before closing the discussion on separation, the importance of D in the determination of the separation point should be discussed. The coefficients in the expression for A are such that, for fixed Reynolds number, Mach number, and deflection angle, the magnitude of A increases as D increases. The separation point has been seen to move upstream as A is increased in magnitude, hence an overestimation of the downstream thickening would result in a slight overestimation of the upstream distance to the separation point. In figure 9 the variation of separation point for different Mach numbers has been plotted for fixed Reynolds number. The location of the separation point for the case $D = 0$ has also been plotted in this figure. These curves thus give the greatest lower bound of the separation distance since it is known that actually $D > 0$. A comparison of results reveals that D has a very small effect upon the location of the separation point. For the higher Mach numbers in the range investigated, the percentage difference between the two cases may be fairly large, but the fact that the separation distance is measured in multiples of a boundary-layer displacement thickness must be

considered. In an actual experimental measurement of the absolute distance to the separation point, this difference will be extremely small. Hence, for practical purposes, one can consider $D = 0$ when estimating the separation point. The results obtained under such conditions will then yield a slight underestimation of the separation point.

Pressure Distribution

The pressure disturbance along the wall (fig. 10) decays exponentially from a definite value at the point of incidence to zero far upstream of that point. Downstream of the point of incidence the pressure rises to a maximum value before dropping to the value corresponding to regular reflection. This downstream overcompression has been observed experimentally, and it appears to be a characteristic feature of shock-wave interaction with a laminar boundary layer. The Lees' theory, as mentioned previously, failed to predict this downstream behavior. This is due to the fact that an incomplete solution for the pressure was used in the determination of the pressure distribution. The boundary layer was divided, longitudinally, into four regions, and it was assumed that the solutions to a third-order differential equation were valid in each region. In the two regions that extended to positive and negative infinity, certain solutions could be rejected since they became infinite at the ends of their respective regions. In the finite regions, however, the complete solutions must be retained. The incompleteness of the Lees' theory, then, arises from the fact that only one term of the general solution was used in each of the finite regions.

The linear theory yields pressure distributions that are similar irrespective of the size of the deflection angle. Now for very small angles, the experimental results exhibit the general behavior predicted by theory. In figure 10 the experimental values of the pressure distribution have been plotted for $\epsilon = 1^\circ$ and $M_\infty = 2.05$. (In this case, separation has probably not occurred since the wave is quite weak.) The values of the pressure ratio were taken from figure 13 of reference 4 and converted to the scale indicated. The upstream portion of this curve can be well represented by an exponential curve, thus verifying, at least for this case, the predicted exponential pressure rise. For larger deflection angles, the experimental pressure distributions are characterized by the familiar pressure "bump" ahead of the point of incidence, thus indicating that separation has occurred. The linear theory is inadequate, as regards predicting this upstream behavior; hence for large deflection angles the theory must be modified, possibly by taking account of the second-order effects upstream of the point of incidence.

SHOCK-WAVE INTERACTION WITH A TURBULENT BOUNDARY LAYER

Method of Approximations

When the flow in the boundary layer is turbulent, the Kármán momentum-integral equation will take on the same form as for the laminar boundary layer except that the quantities involved are not the exact, but average, values. However, since general relationships between the shear stress and the mean velocity in turbulent layers have not yet been established, rigorous treatment of the problem at this time is, of course, not possible. Here, for the purpose of exhibiting the characteristic difference between the laminar and turbulent cases, certain approximations are proposed.

The momentum-integral equation expresses the shear stress at the wall in terms of the growth of the boundary-layer momentum thickness and the velocity gradient. Using experimental results as a guide, the relative importance of these terms can be estimated. Experimental results of Fage and Sargent (reference 18) show that the shear stress in front of the shock is practically constant; behind the shock, it is very small. Therefore, unlike the laminar case, the shear stress to the first approximation, both in front of and behind the shock, can be regarded as constant and hence has no effect on the perturbed flow. It follows then that, in the case of a turbulent boundary layer, the growth of the momentum thickness is influenced primarily by pressure changes due to the presence of the shock.

To simplify the problem further, it is noted, for practical purposes, that the shape parameter $H \equiv \delta^*/\theta$ is relatively insensitive to change even though there may be a considerable adverse pressure gradient. In the transonic case, where there is a normal shock in the local supersonic region and a large change in H is anticipated, H at its maximum is only increased by a factor of about 1.2 (see reference 2). The reason for this is possibly the fact that the increase by the shock may be counterbalanced by a decrease due to compressibility effect. Moreover, in the momentum-integral equation, the coefficient of the velocity gradient is positive and usually greater than unity within the Mach number range; hence one can ignore the slight variation in H and consider it a constant. By the same token, the Mach number in this coefficient can also be considered to be constant. (The Mach number enters when the density is eliminated in terms of the velocity.) Consequently, the momentum-integral equation reduces to:

$$\frac{d \Delta}{dx} + \alpha_3 \frac{du'}{dx} = 0$$

where

$$\alpha_3 \equiv 2 + H - M_\infty^2$$

Solution for Outer Flow

Similar to the previous case, for the upstream region $\phi_1 = f(\xi - m_\infty \eta)$. By applying the original condition $d\Delta/d\xi = \partial\phi/\partial\eta$ at $\eta = 0$, there is obtained from the linear theory

$$f = f_0 e^{m_\infty/\alpha_3 (\xi - m_\infty \eta)} + \text{Constant}$$

Since $m_\infty/\alpha_3 > 0$, the disturbances vanish far upstream. When α_3 is evaluated the exponent m_∞/α_3 is found to be about one order larger than λ_2 of the laminar case. This is the well-known experimental result that there is very little upstream influence in the turbulent case. This, therefore, confirms the hypotheses made in the previous section.

For the downstream solution

$$\phi_3 = g(\xi - m_\infty \eta) - \frac{\epsilon}{m_\infty}(\xi + m_\infty \eta)$$

The original differential equation remains the same; hence the downstream solution would be

$$\phi_3 = g_0 e^{m_\infty/\alpha_3 (\xi - m_\infty \eta)} - \frac{2\epsilon}{m_\infty} \xi + \text{Constant}$$

It shows that if the solution ϕ_1 is continued to the downstream side the velocities would become infinite at positive infinity and must be rejected. There is therefore a principal difference between the laminar and turbulent cases. In the laminar case several solutions for the outer flow were obtained and the solution appropriate for either upstream or downstream could be chosen. In the turbulent case there is no choice since there is only one solution for the outer flow, which, if continued, fails at positive infinity. This indicates that linearization of the flow is incapable of accounting for the flow near the point of incidence where the nonlinear effects become important. Since large changes in flow velocities can be brought about only through a shock, in the present problem a reflected shock must be considered.

From general considerations it can be argued that if one puts a shock wave between regions 2 and 3 and considers perturbations of a regular reflection it may be possible to obtain a solution which will satisfy the conditions at infinity. By perturbing the regular reflection, there would be, in each region, undisturbed quantities plus their perturbations. Consider the total potential in region 3:

$$\phi_3 = \xi + f(\xi - m_3 y) + g(\xi + m_3 y)$$

At infinity $f' = g' = 0$; along the reflected wave $\xi - m_3 \eta = 0$, to first order, the velocities are constant; hence

$$f' \pm g' = \text{Constant}$$

But to first order, along the wave, $f'(0) = \text{Constant}$; hence $g'(\xi) = \text{Constant}$. Therefore, $g'(\xi)$ is constant throughout region 3. But $g' = 0$ at infinity; hence $g' = 0$ in region 3.

Then at the boundary layer $d\Delta/d\xi = -m_3 f'(\xi)$ where f is nondimensional, and the substitution into the momentum-integral equation yields

$$-m_3 f' + \alpha_3 f'' = 0$$

$$f = \text{Constant} + f_0 e^{m_3/\alpha_3 \xi}$$

$$f' = f_0 \frac{m_3}{\alpha_3} e^{m_3/\alpha_3 \xi}$$

Now $f' = 0$ at infinity; hence one must choose $f_0 = 0$; and thus

$$f = \text{Constant}$$

This means that behind the reflected shock, the flow, to the first order, is uniform. Since the flow behind the incident shock has undergone compression up to the reflected wave, it can be seen that, to satisfy the condition at infinity, the reflected shock must be followed by a very rapid expansion. Otherwise, the pressure after the second shock would have been higher than that after the regular reflection. It is therefore concluded that in the case of a turbulent boundary layer the incident shock is reflected as a shock and behind the reflected shock there

must be an abrupt expansion so as to cancel the overcompression brought about by the train of upstream compression waves. The existence of the sharp expansion behind the reflected shock was also confirmed by experiments (reference 9). The pressure distribution and boundary-layer growth, to the first order, appear to be discontinuous as shown in figure 12.

Downstream Thickening for Turbulent Boundary Layers

The downstream thickening can be estimated by use of the formula

$$\frac{\delta_3^*}{\delta_1^*} = \frac{\rho_1}{\rho_3} \left(\frac{u_1}{u_3} \right)^{2+H}$$

Now the difference between the laminar and turbulent cases is that H differs for the two cases. Since, in general, $H_t < H_l$, the downstream thickening in the turbulent case is less than the thickening in the corresponding laminar case. Empirical relations must be relied on to estimate H because of the lack of knowledge of the compressible turbulent boundary layer. According to Nitzberg and Crandall (reference 19), for local Mach numbers greater than the free-stream Mach number, but less than 1.4, the compressibility effect is well approximated by

$$H = H_{M=0} \left(1 + \frac{2}{5} M^2 \right)$$

Use this relationship to estimate the downstream thickening and then compare the results with the existing experimental data. By assuming a 1/7-power law for the incompressible profile,

$$H = 1.29 \left(1 + 0.4 M_\infty^2 \right)$$

The predicted thickening is shown in figure 13. It shows that the downstream thickening increases as the Mach number is decreased. This behavior is also present in the laminar case.

Using this value of H , it was found that the predicted thickening for $M_\infty = 1.44$ and $\epsilon = 4.5^\circ$ is larger than the visually estimated thickening in the experimental case. On the other hand, the predicted thickening for $M_\infty = 2$ and $\epsilon = 6^\circ$ is slightly less than the visually estimated thickening in the experimental case. It should be noted, however, that, for $M > 1.4$, a relationship has been used that is supposedly

valid for $M < 1.4$. Moreover, this relationship merely accounts for the effects of compressibility. It would appear that some effect of the shock must also be included in the determination of H . However, at this time, owing to the lack of exact information, it must be neglected. Consequently, it appears that if the relation $H = 1.29(1 + 0.4M_\infty^2)$ is used for Mach numbers not too much larger than 1.4, one can expect to have a minimum estimate of the downstream thickening.

SUMMARY OF RESULTS

An investigation of the reflection of a weak shock wave from a boundary layer along a flat plate yielded the following results.

Laminar Case

1. In all cases investigated, the pressure along the wall overcompresses downstream of the point of incidence. The pressure disturbance decays exponentially from a definite value at the point of incidence to zero far upstream of the point of incidence. Downstream, the pressure rises to a maximum value and then falls, gradually, to the constant value corresponding to regular reflection.

The exponential pressure rise appears to be verified in the case of a shock deflection angle of 1° , since separation has probably not occurred. For larger deflection angles (the next larger angle for which there are experimental pressure distributions is 3°), the experimental pressure distributions exhibit the familiar pressure bump between the separation point and the origin. For these angles, a true comparison between experimental results and theoretical results cannot be made since the present theory does not account for the effects of separation.

2. If the upstream influence is considered to be the distance to the point at which the disturbance has decayed to a specified fraction of its amplitude at the origin, the upstream influence, when measured in multiples of the boundary-layer displacement thickness δ_o^* , is found to increase with increasing Reynolds number: $x/\delta_o^* \propto (Re/m_\infty)^{1/2}$ where x is the coordinate parallel to the flow direction, Re is the Reynolds number, $m_\infty = \sqrt{M_\infty^2 - 1}$, and M_∞ is the free-stream Mach number. For decreasing Mach number, the upstream influence also increases. If the disturbance is considered to decay to, say, 5 percent of its amplitude at the origin, the upstream influence for $M_\infty \approx 2$ and $Re \approx 1500$ is of the order of 30 boundary-layer displacement thicknesses.

3. The pressure gradient is such that the boundary layer may separate ahead of the point of incidence. In the event of separation, an increase of shock strength, for fixed Mach numbers and Reynolds number, increases the distance between the separation point and the point of incidence. For fixed Mach number and shock-deflection angle, the separation point measured in multiples of δ_0^* moves upstream with increasing Reynolds number. For the case of $M_\infty = 1.44$ and $Re = 2000$, the boundary layer separates for all flow-deflection angles $\epsilon > 1.03^\circ$.

For fixed Reynolds number and shock-deflection angle, the separation point, measured in multiples of δ_0^* , moves upstream with decreasing Mach number.

For a complete determination of the constants of integration, an estimate of the downstream boundary-layer thickness was required. For the cases investigated, the effect of the downstream thickening on the outer flow is rather small. In fact, for practical purposes, this effect of downstream thickening can be neglected in the determination of the separation point. The distance between the origin and the separation point will then be slightly underestimated.

4. The present theory is applicable only in the case when a weak shock is incident upon a laminar boundary layer. In addition to the outer flow field, the boundary-layer displacement thickness has also been linearized. The latter linearization enables a linear differential equation with constant coefficients to be obtained for the perturbation velocity potential. This equation immediately yields the general solution of the outer flow. Upon investigating the size of the perturbations, the maximum velocity perturbations are found to be about 10 percent or less. The thickness perturbations, on the other hand, are much larger, being about 30 percent near the origin; thus the linearization of the displacement thickness becomes questionable as the point of incidence is approached. Had the displacement thickness not been linearized, a rather complicated nonlinear differential equation would have been obtained from the boundary condition for the perturbation velocity potential. A solution of this equation would be expected to yield more accurate results. However, it is problematical as to whether the equation could be solved without the imposition of additional assumptions which, in themselves, might nullify any accuracy that the nonlinear boundary condition may provide.

Turbulent Case

In the case of shock-wave interaction with a turbulent boundary layer the upstream influence is found to be considerably less than in the laminar case. In addition, to first order, the incident wave must

be reflected as a compression wave followed immediately by an expansion wave, so that the end pressure condition is satisfied.

Cornell University

Ithaca, N. Y., January 11, 1952

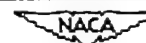
REFERENCES

1. Ferri, Antonio: Experimental Results with Airfoils Tested in the High-Speed Tunnel at Guidonia. NACA TM 946, 1940.
2. Ackeret, J., Feldmann, F., and Rott, N.: Investigations of Compression Shocks and Boundary Layers in Gases Moving at High Speed. NACA TM 1113, 1947.
3. Liepmann, H. W., Roshko, A., and Dhawan, S.: On the Reflection of Shock Waves From Boundary Layers. NACA TN 2334, 1951.
4. Barry, F. W., Shapiro, A. H., and Neumann, E. P.: The Interaction of Shock Waves with Boundary Layers on a Flat Surface. Jour. Aero. Sci., vol. 18, no. 4, April 1951, pp. 229-239.
5. Howarth, L.: The Propagation of Steady Disturbances in a Supersonic Stream Bounded on One Side by a Parallel Subsonic Stream. Proc. Cambridge Phil. Soc., vol. 44, pt. 3, July 1947, pp. 380-390.
6. Tsien, Hsue-Shen, and Finston, Morton: Interaction Between Parallel Streams of Subsonic and Supersonic Velocities. Jour. Aero. Sci., vol. 16, no. 9, Sept. 1949, pp. 515-528.
7. Robinson, A.: Wave Reflection near a Wall. Rep. No. 37, The College of Aero., Cranfield, May 1950.
8. Lighthill, M. J.: Reflection at a Laminar Boundary Layer of a Weak Steady Disturbance to a Supersonic Stream, Neglecting Viscosity and Heat Conduction. Quart. Jour. Mech. and Appl. Math., vol. III, pt. 3, Sept. 1950, pp. 303-325.
9. Bardsley, O., and Mair, W. A.: The Interaction between an Oblique Shock-Wave and a Turbulent Boundary-Layer. Phil. Mag., ser. 7, vol. XLIII, no. 42, Jan. 1951, pp. 29-36.
10. Lees, Lester: Interaction between the Laminar Boundary Layer over a Plane Surface and an Incident Oblique Shock Wave. Rep. No. 143, Contract N6ori-270, Task Order No. 6, Office of Naval Research, Contract NOrd-7920, Task No. PRN-2-E, Bur. Ord., U. S. Navy, and Aero. Eng. Lab., Princeton Univ., Jan. 24, 1949.
11. Oswatitsch, K., and Wieghardt, K.: Theoretical Analysis of Stationary Potential Flows and Boundary Layers at High Speed. NACA TM 1189, 1948.

12. Kuo, Yung-Huai: Reflection of a Weak Shock Wave from a Boundary Layer along a Flat Plate. II - Interaction of Oblique Shock Wave with a Laminar Boundary Layer Analyzed by Differential-Equation Method. NACA TN 2869, 1953.
13. Howarth, Leslie: Concerning the Effect of Compressibility on Laminar Boundary Layers and Their Separation. Proc. Roy. Soc., (London), ser. A, vol. 194, no. 1036, July 1948, pp. 16-42.
14. Emmons, Howard W., and Brainerd, John Grist: Temperature Effects in a Laminar Compressible-Fluid Boundary Layer along a Flat Plate. Jour. Appl. Mech., vol. 8, no. 3, Sept. 1941, pp. A-105 - A-110.
15. Brainerd, J. G., and Emmons, H. W.: Effect of a Variable Viscosity on Boundary Layers, with a Discussion of Drag Measurements. Jour. Appl. Mech. vol. 9, no. 1, March 1942, pp. A-1 - A-6.
16. Crocco, Luigi: Lo strato limite laminare nei gas. Monografie Scientifiche di Aeronautica. No. 3, Ministero della Difesa-Aeronautica, Roma, Dec. 1946.
17. Ritter, A.: On the Reflection of a Weak Shock Wave from a Boundary Layer along a Flat Plate. Thesis, Cornell Univ., 1951.
18. Fage, A., and Sargent, R. F.: Shock Wave and Boundary Layer Phenomena near a Flat Surface. Proc. Roy. Soc. (London), ser. A, vol. 190, no. 1020, June 17, 1947, pp. 1-20.
19. Nitzberg, Gerald E., and Crandall, Stewart: Some Fundamental Similarities between Boundary-Layer Flow at Transonic and Low Speeds. NACA TN 1623, 1948.
20. Lees, Lester: The Stability of the Laminar Boundary Layer in a Compressible Fluid. NACA Rep. 876, 1947.
21. Stewartson, K.: Correlated Incompressible and Compressible Boundary Layers. Proc. Roy. Soc. (London), ser. A, vol. 200, no. 1060, Dec. 22, 1949, pp. 84-100.

TABLE I
COEFFICIENTS USED IN DETERMINING CONSTANTS OF INTEGRATION

M_∞	$Re = \frac{U_0^*}{\nu_0}$	$\frac{-(\lambda_3 + \lambda_1)}{(\lambda_2 - \lambda_3)(\lambda_2 - \lambda_1)}$	$\frac{\lambda_1 \lambda_3}{(\lambda_2 - \lambda_3)(\lambda_2 - \lambda_1)}$	$\frac{(\lambda_3 + \lambda_2)}{(\lambda_3 - \lambda_1)(\lambda_2 - \lambda_1)}$	$\frac{-\lambda_2 \lambda_3}{(\lambda_3 - \lambda_1)(\lambda_2 - \lambda_1)}$	$\frac{-(\lambda_2 + \lambda_1)}{(\lambda_3 - \lambda_1)(\lambda_2 - \lambda_3)}$	$\frac{\lambda_1 \lambda_2}{(\lambda_3 - \lambda_1)(\lambda_2 - \lambda_3)}$
1.44	250	2.970	0.0642	0.965	0.0250	2.020	-0.961
	500	3.810	.0435	1.771	.0225	2.370	-.980
	1000	4.880	.0282	2.822	.0179	2.050	-.989
	2000	6.600	.0192	4.360	.0136	2.230	-.977
2	250	1.103	0.0546	0.747	0.0453	0.357	-0.992
	500	1.575	.0439	1.168	.0385	.408	-.994
	1000	2.182	.0330	1.815	.0311	.369	-.998
	2000	3.070	.0235	2.675	.0224	.396	-.999
2.5	250	0.402	0.0366	0.698	0.0785	-0.295	-1.043
	500	.651	.0363	1.038	.0706	-.386	-1.034
	1000	1.018	.0326	1.472	.0558	-.455	-1.022
	2000	1.540	.0287	2.025	.0434	-.488	-1.015



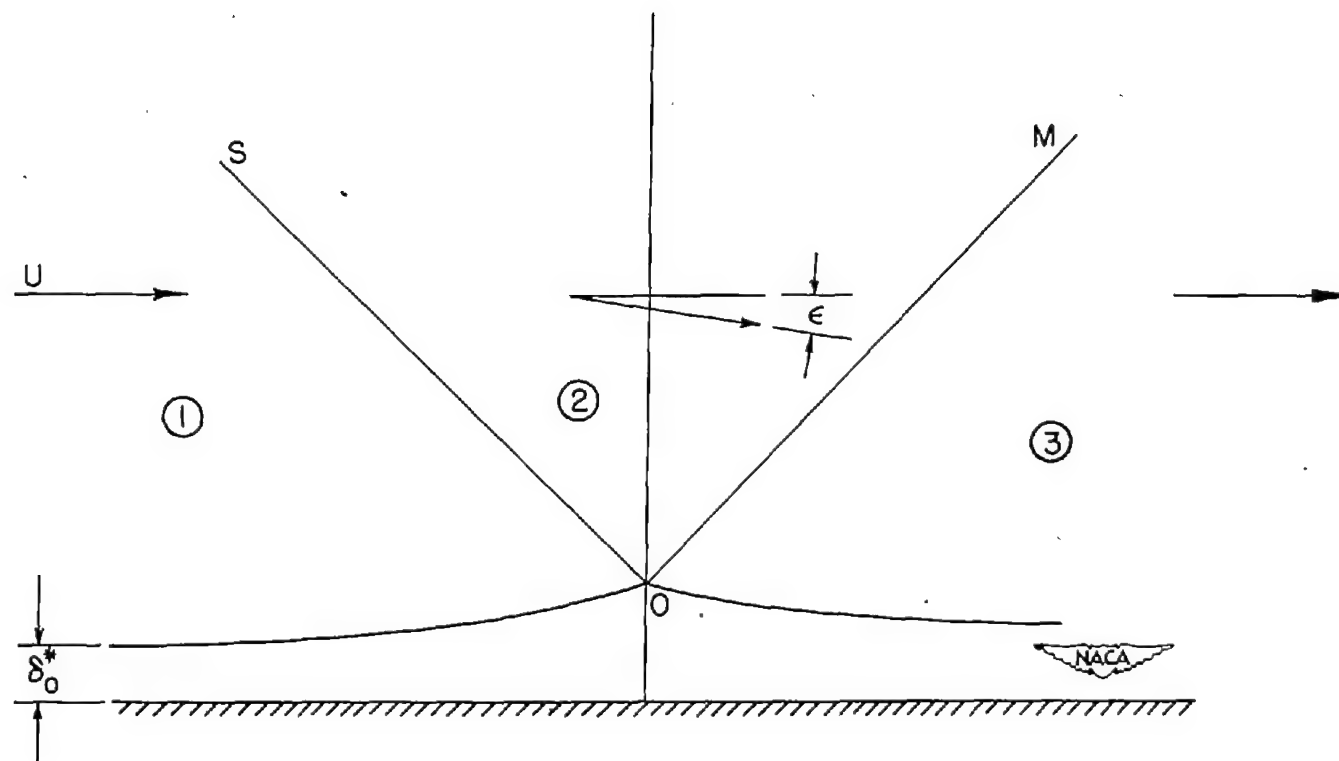


Figure 1.- Simplified model of shock-wave boundary-layer interaction.

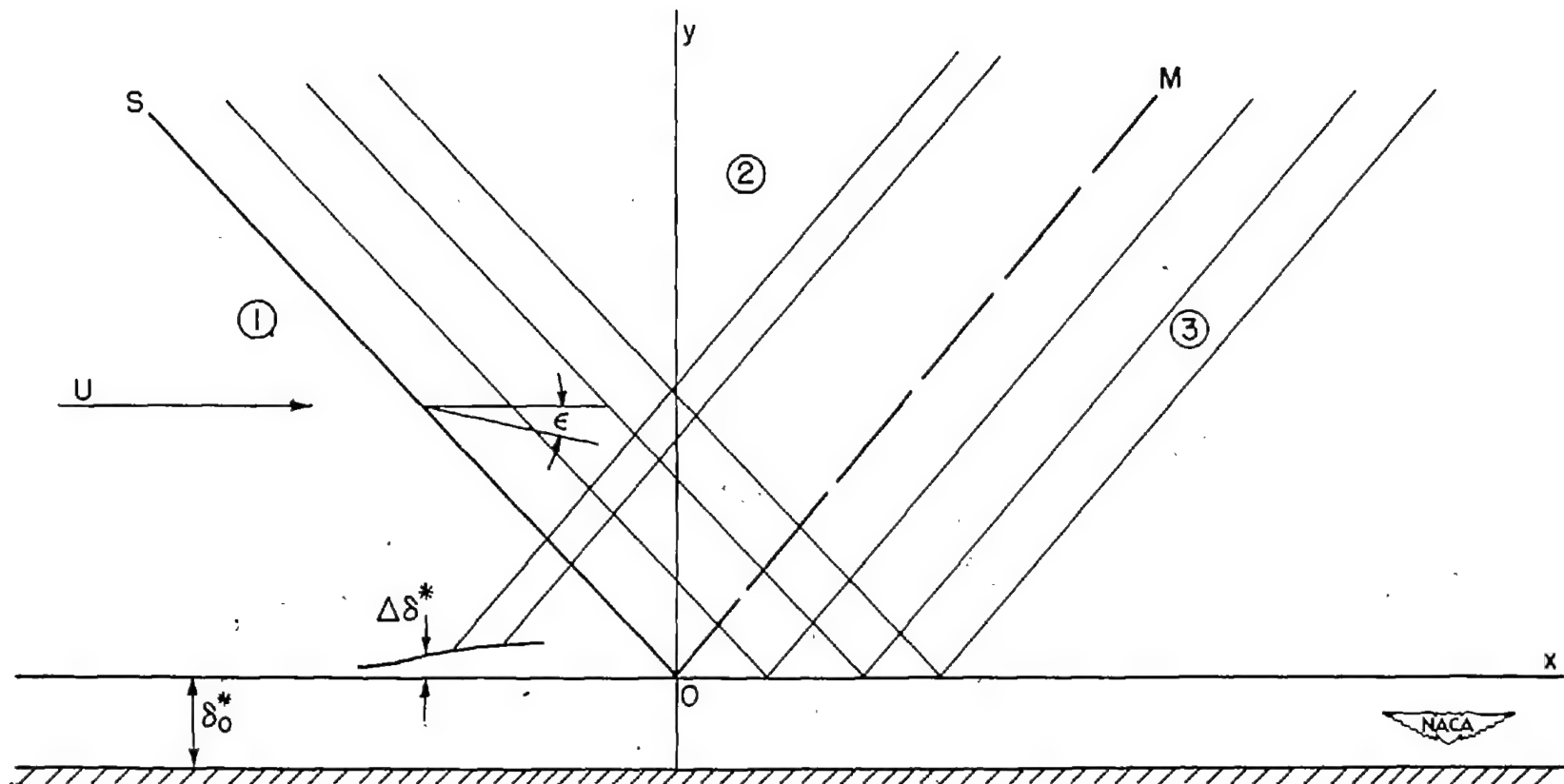


Figure 2.- Shock-wave boundary-layer interaction showing choice of axes.

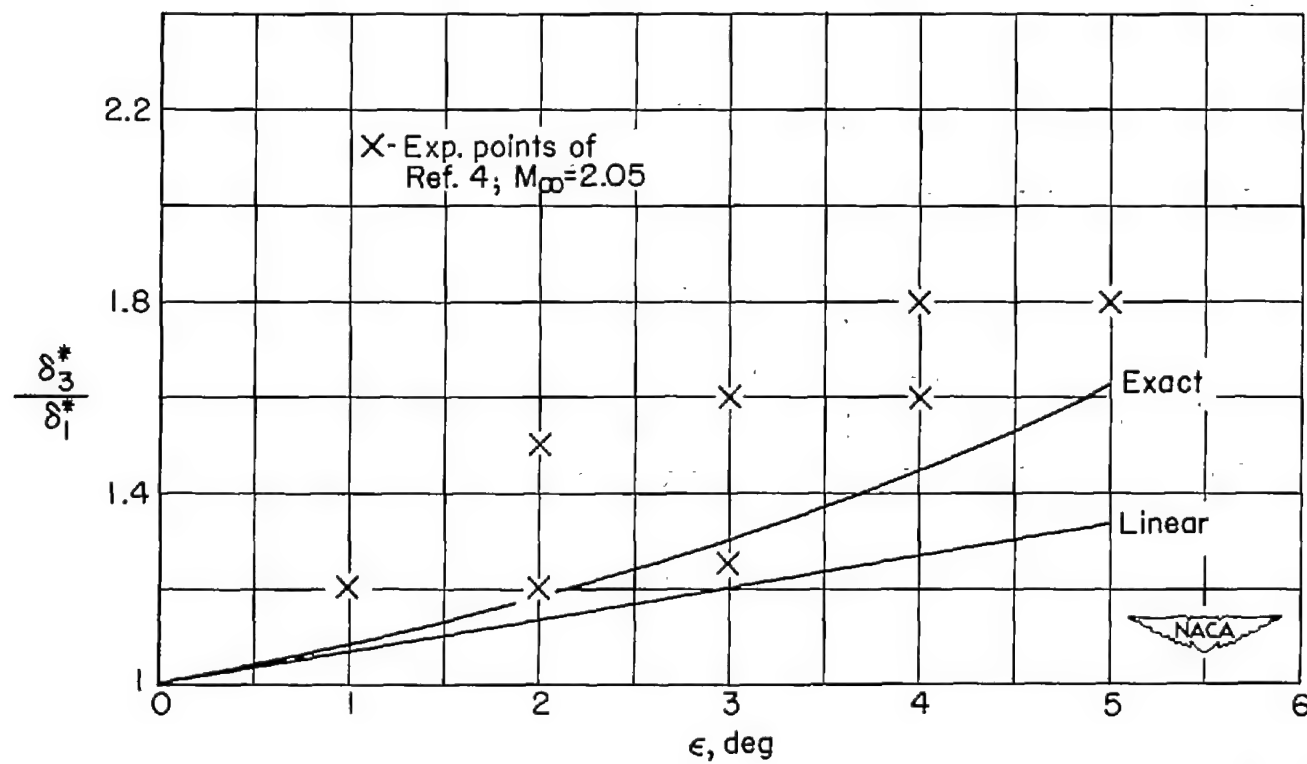


Figure 3.- Displacement-thickness ratio. Laminar case; $M_\infty = 2$;

$$\frac{\delta_3^*}{\delta_1^*} = \frac{\rho_1}{\rho_3} \left(\frac{u_1}{u_3} \right)^{2+H}; \text{ and } H = 2.50 + 3.50 \left(\frac{\gamma - 1}{2} \right) M_\infty^2.$$

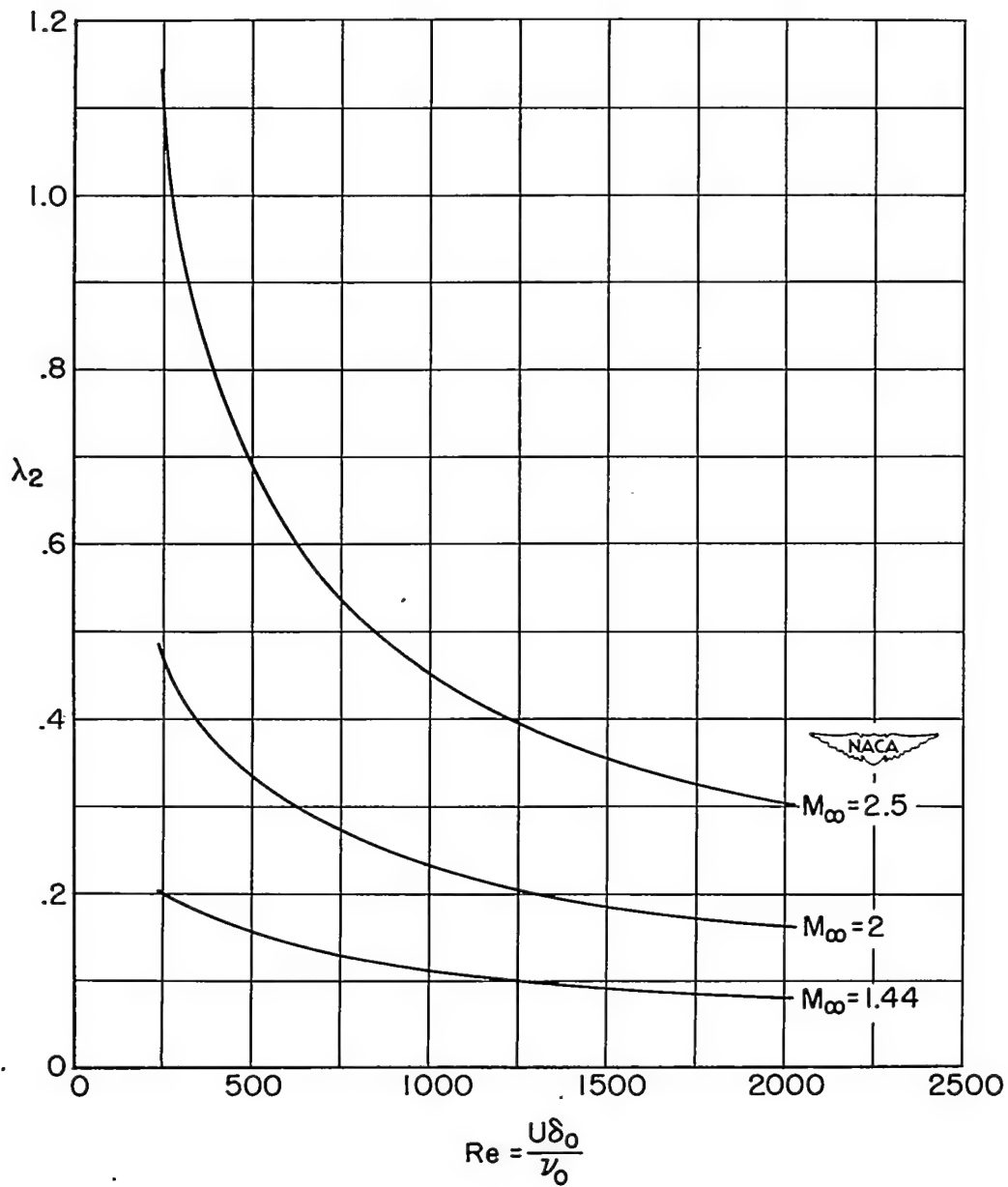
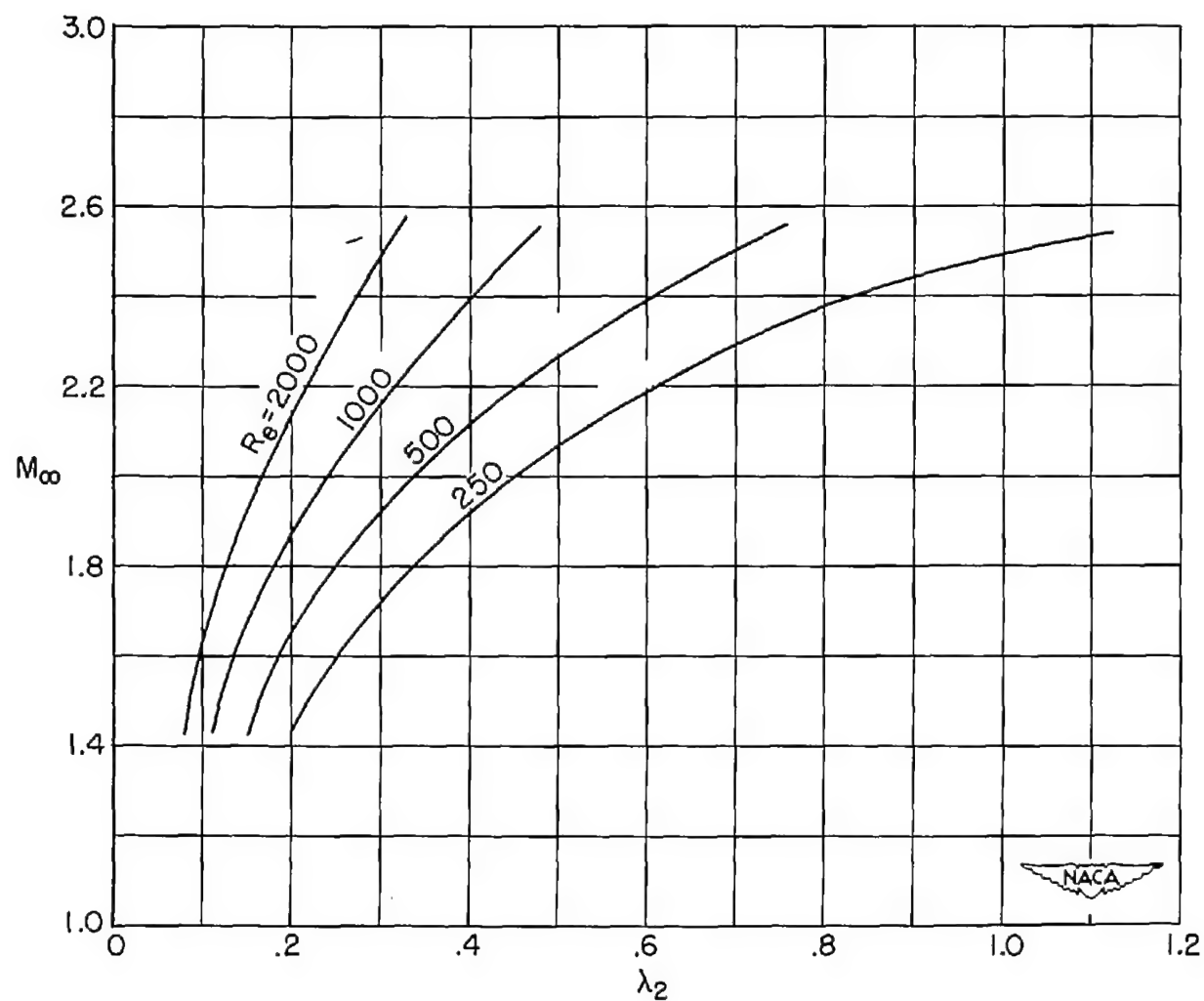
(a) Various values of M_∞

Figure 4.- Measure of upstream influence. $x_d/\delta_0^* = -\frac{1}{\lambda_2} \log_e (1/\alpha)$;
disturbance at x_d/δ_0^* is α percent of disturbance at origin.



(b) Various values of Re .

Figure 4.- Concluded.

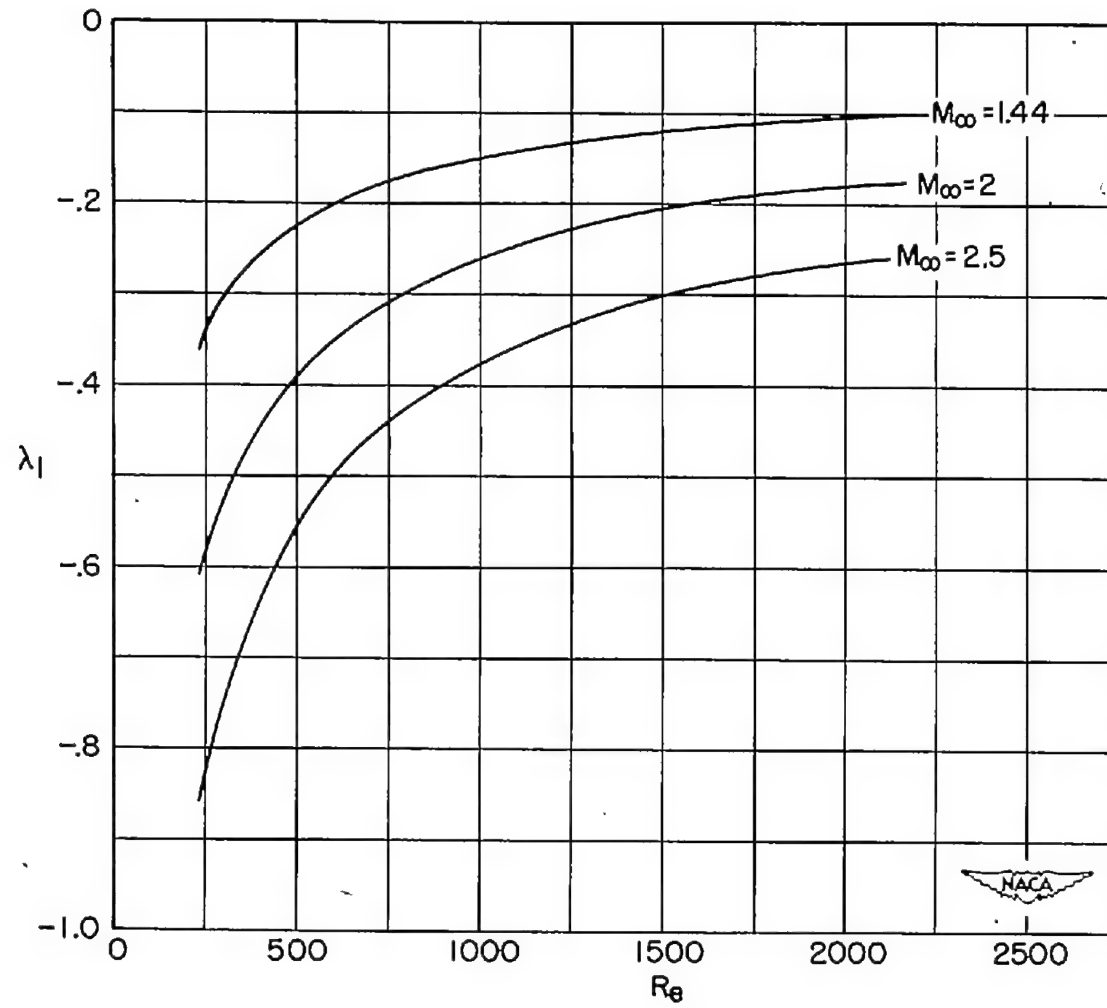


Figure 5.- Reynolds number against λ_1 . $Re = U\delta_0^*/\nu_0$.

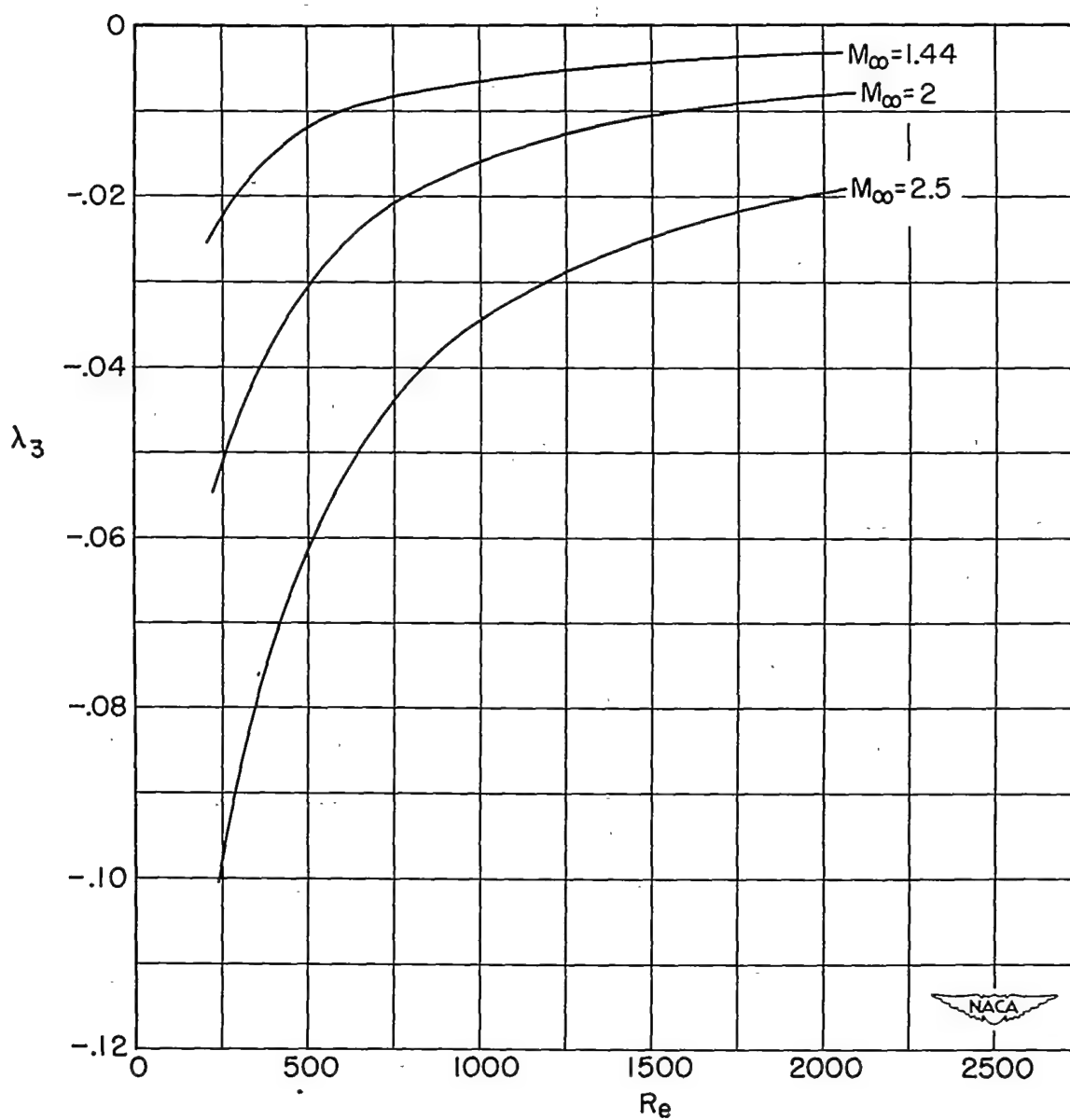


Figure 6.- Reynolds number against λ_3 . $Re = U\delta_o^*/v_o$.

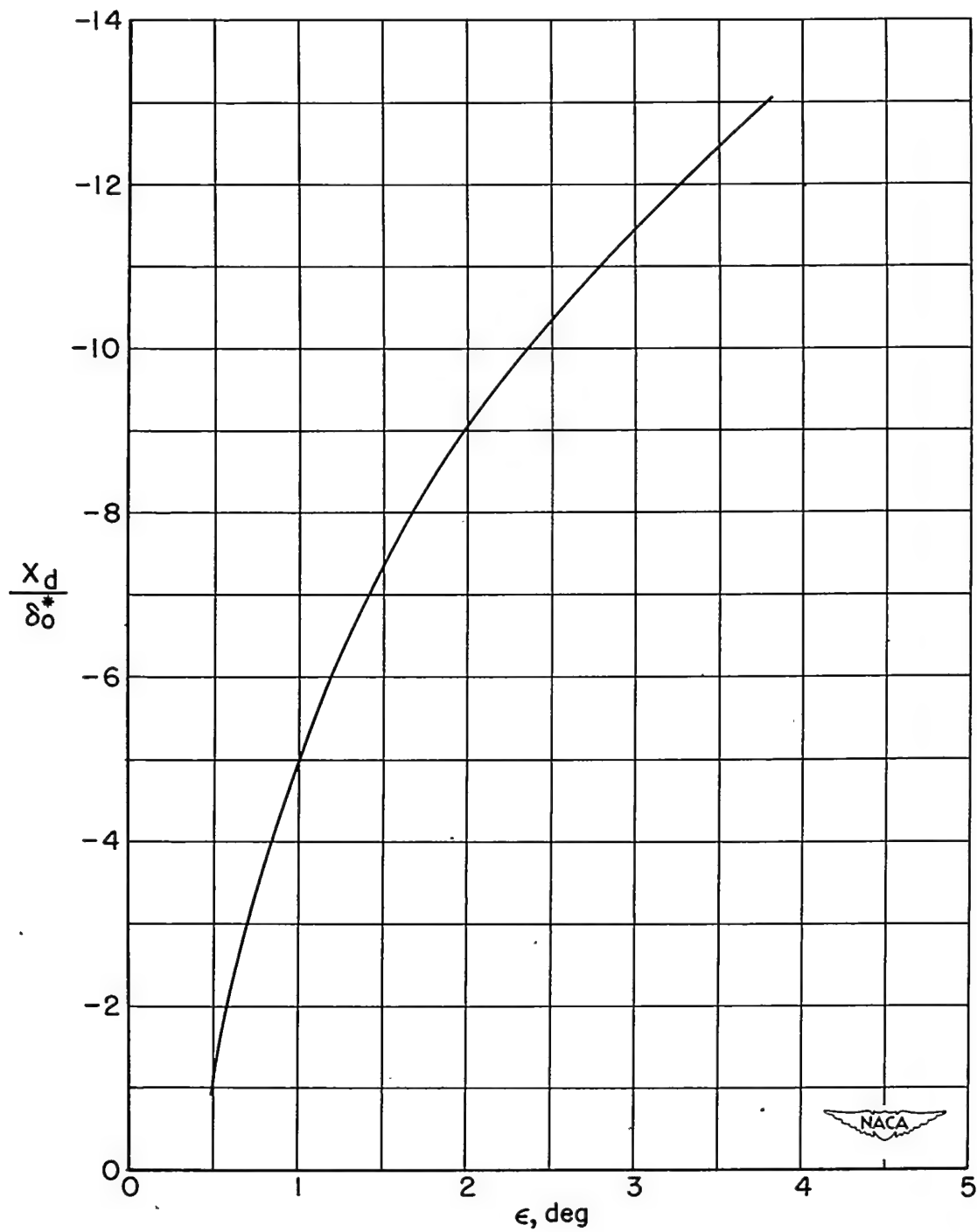


Figure 7.- Upstream influence against deflection angle. $M_\infty = 2$;
 $Re = U\delta_0^*/\nu_0 = 2000$; and $Re_x = Ux/\nu_\infty \approx 51,600$.

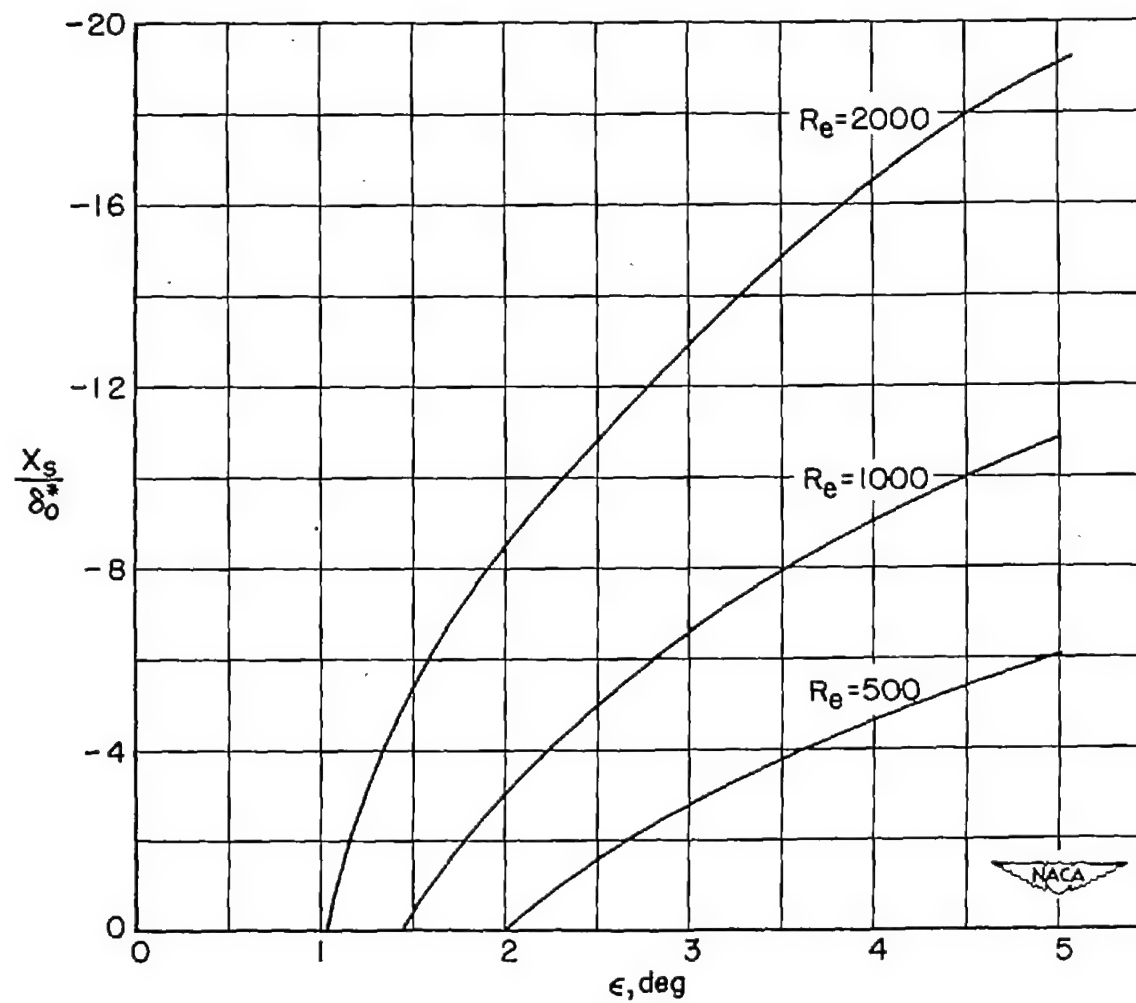


Figure 8.- Separation point against deflection angle. $M_\infty = 1.44$;
 $Re = U\delta_0^*/\nu_0$.

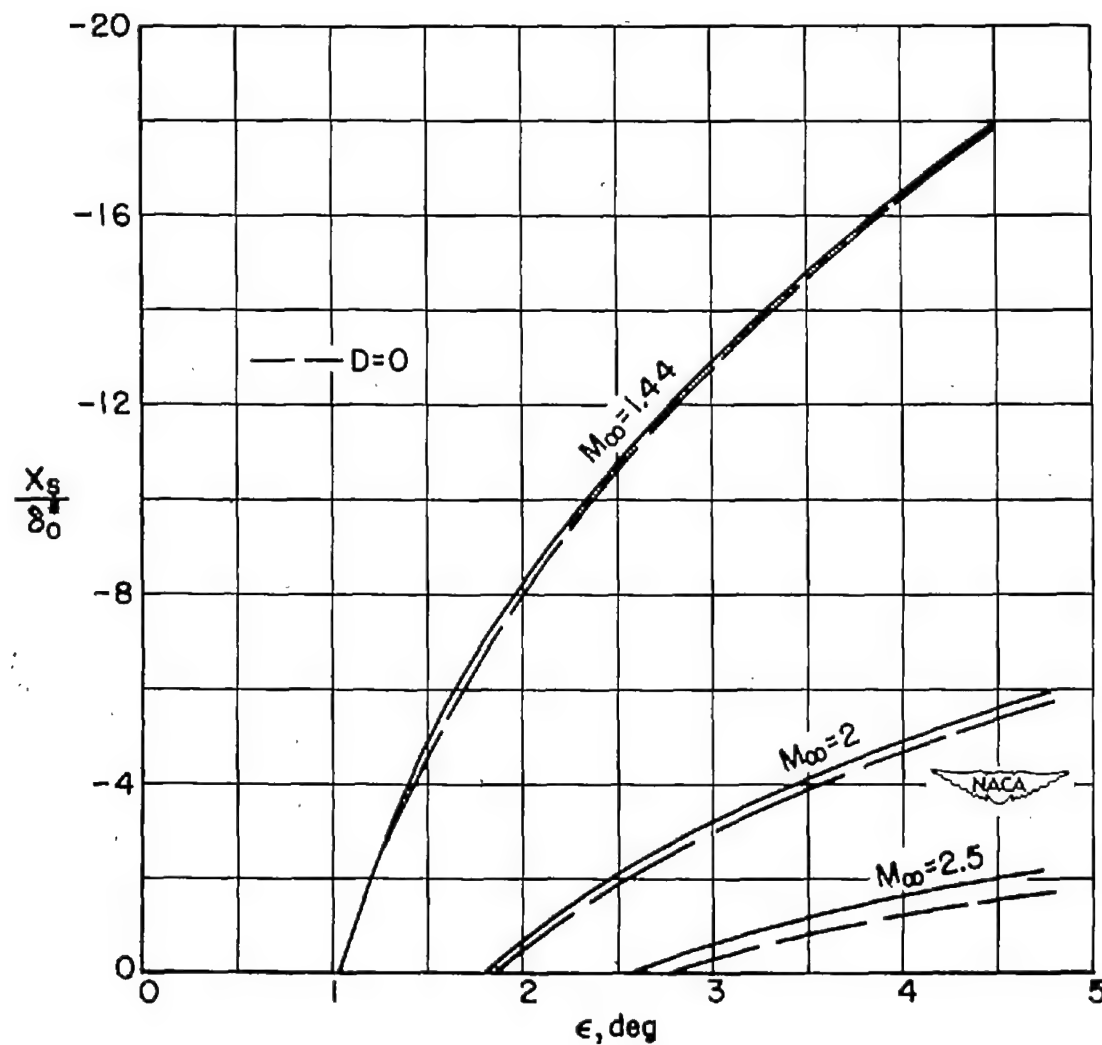


Figure 9.- Separation point against deflection angle. $Re = U\delta_0^*/\nu_0 = 2000$.

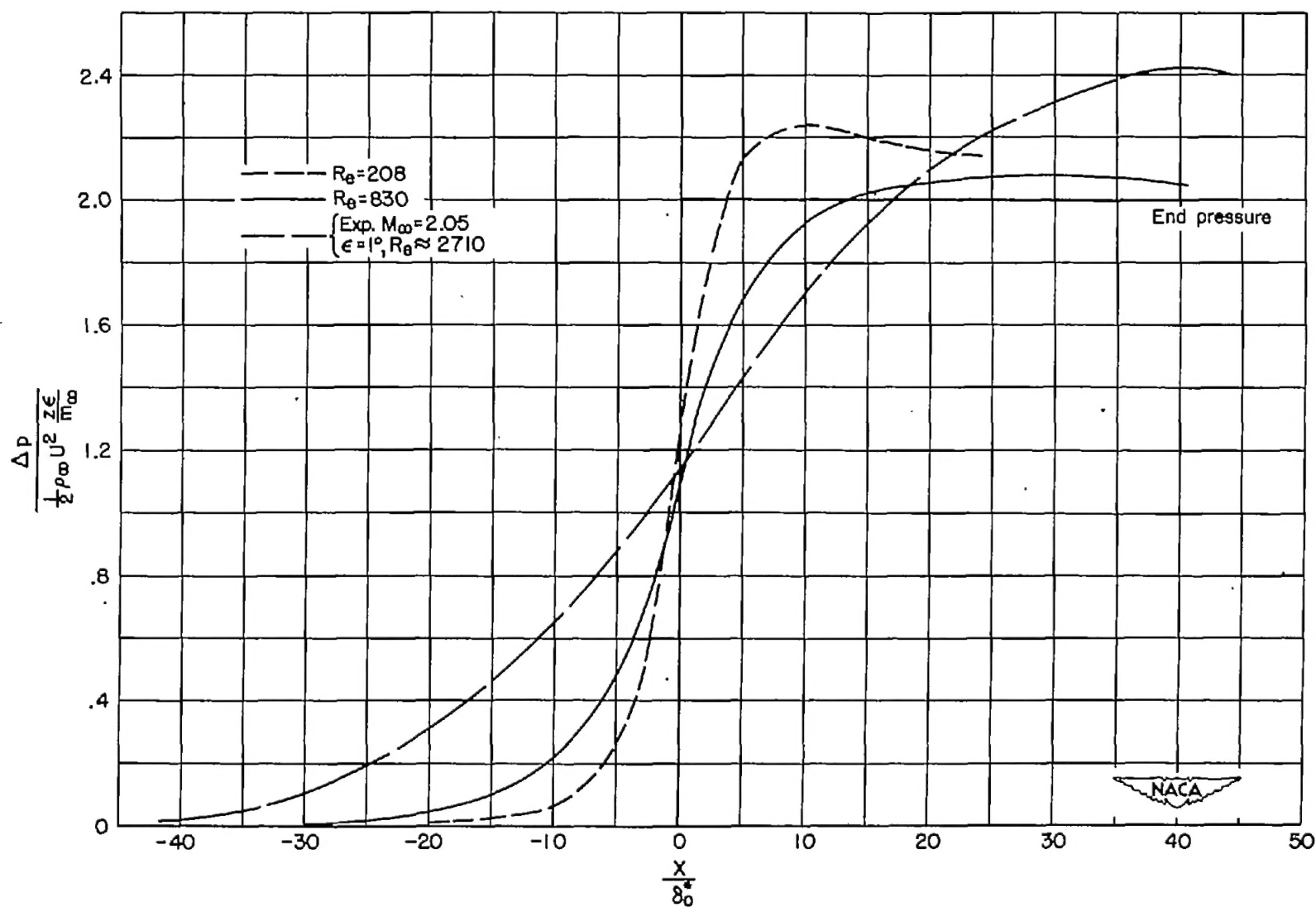


Figure 10.- Wall pressure distribution. $M_{\infty} = 2$; $Re = U\delta_0^*/\nu_{\infty}$.

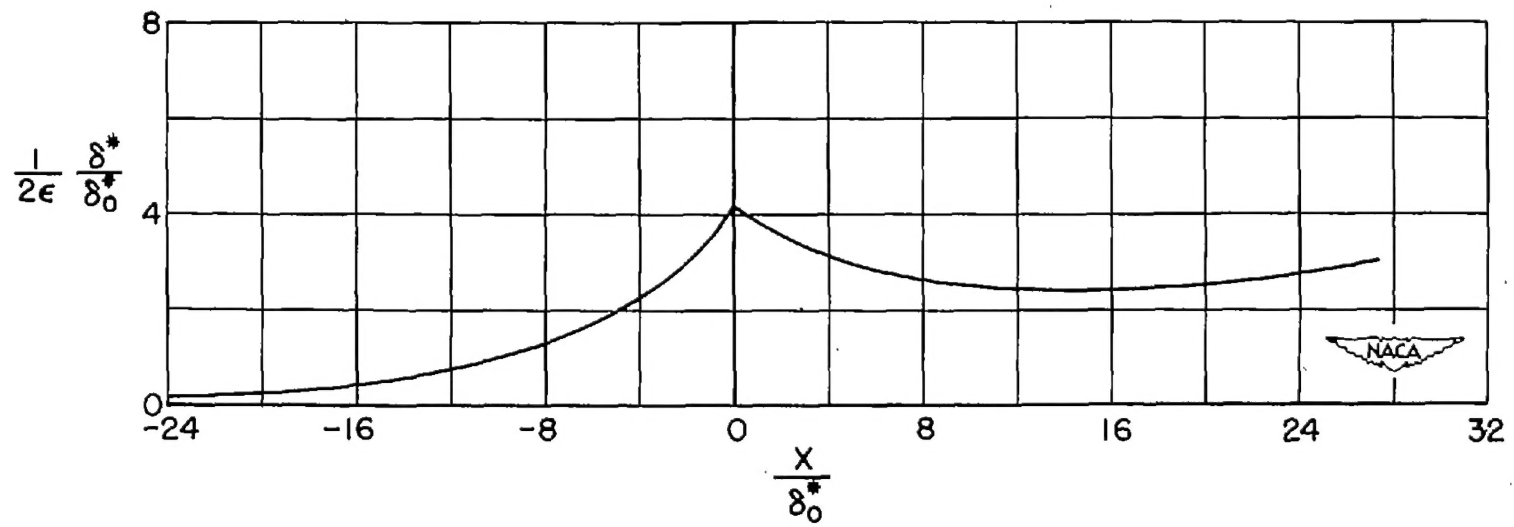


Figure 11.- Perturbed boundary-layer displacement thickness. $M_\infty = 1.44$;
 $Re = U\delta_0^*/\nu_0 = 500$.

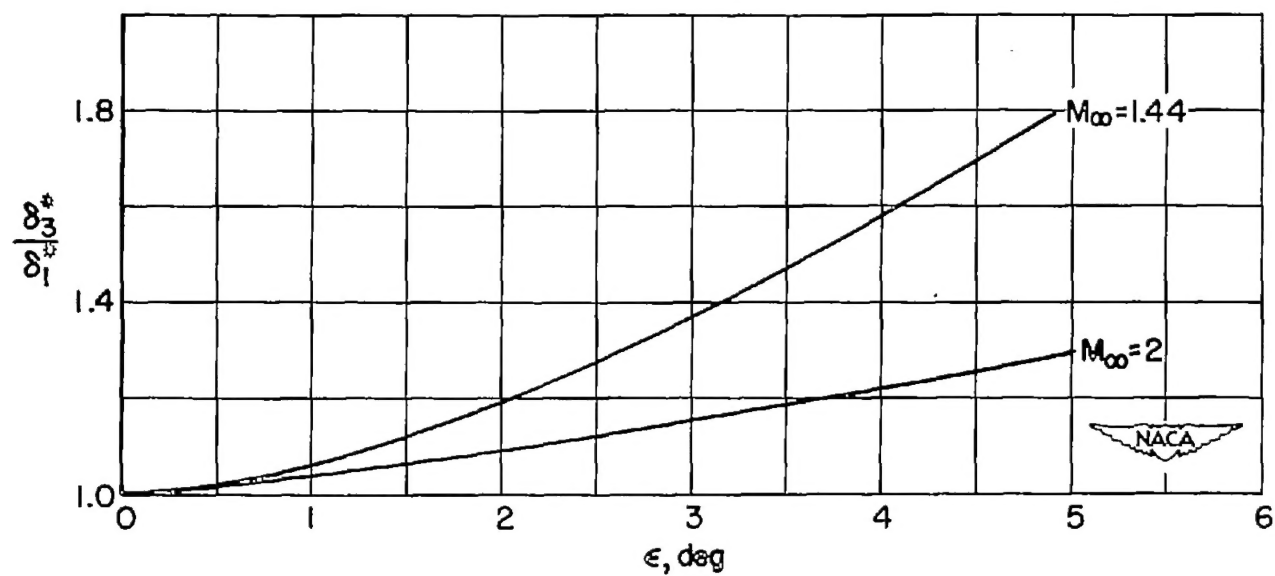


Figure 12.- Downstream thickening turbulent boundary layer.

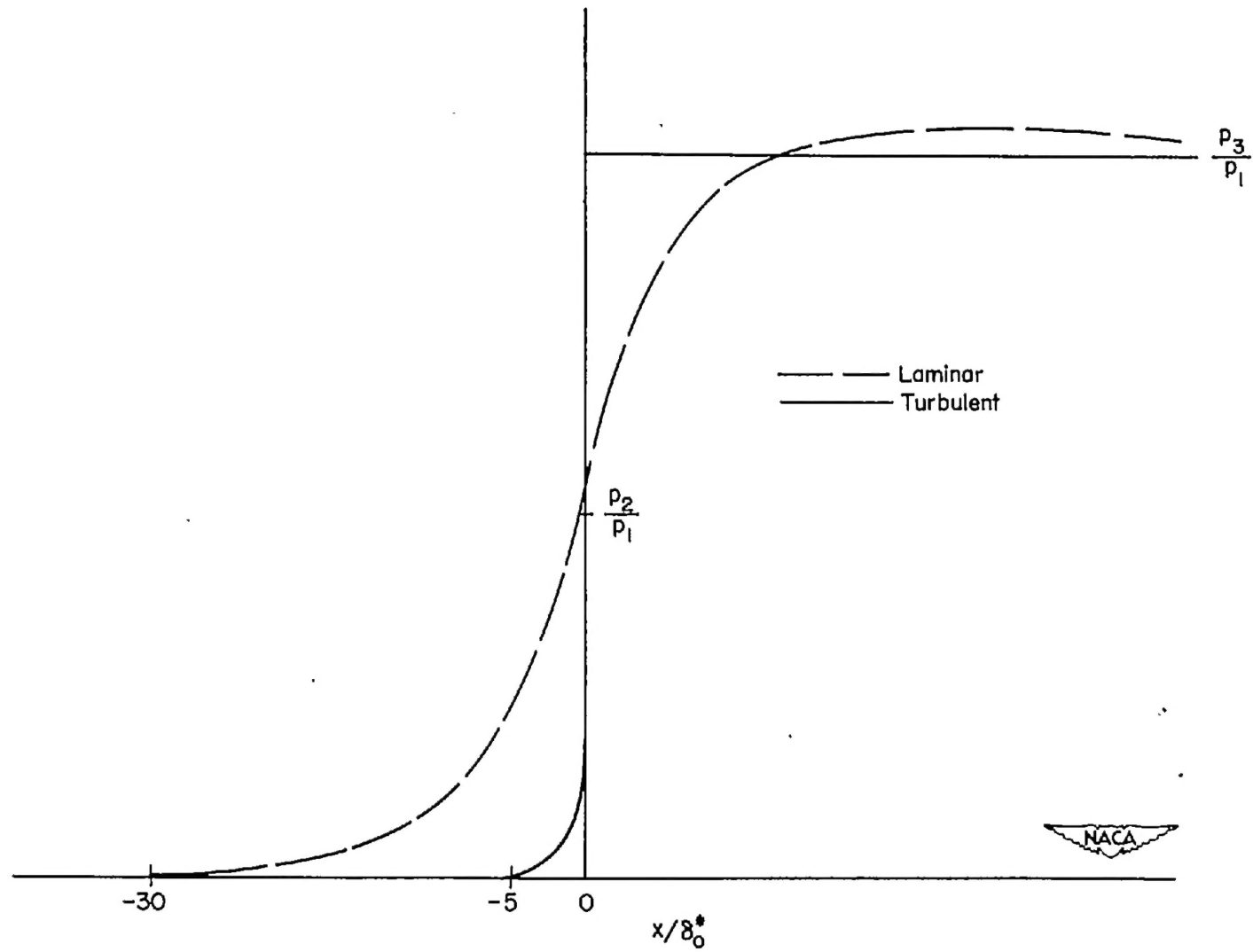


Figure 13.- Wall pressure distribution.